ornl

ORNL/TM-11657

OAK RIDGE
NATIONAL
LABORATORY

MARTIN MARIETTA

Turbo Refrigerating Company Ice Storage Test Report

Therese K. Stovall

OAK RIDGE NATIONAL LABORATORY
CENTRAL RESEARCH LIBRARY
CIRCULATION SECTION
4500N ROOM 175
LIBRARY LOAN COPY
DO NOT TRANSFER TO ANOTHER PERSON
If you wish someone else to see this report, send in name with report and the library will arrange a loan.

MANAGED BY
MARTIN MARIETTA ENERGY SYSTEMS, INC.
FOR THE UNITED STATES
DEPARTMENT OF ENERGY

This report has been reproduced directly from the best available copy.

Available to DOE and DOE contractors from the Office of Scientific and Technical Information, P.O. Box 62, Oak Ridge, TN 37831; prices available from (615) 576-8401, FTS 626-8401.

Available to the public from the National Technical Information Service, U.S. Department of Commerce, 5285 Port Royal Rd., Springfield, VA 22161.

This report was prepared as an account of work sponsored by an agency of the United States Government. Neither the United States Government nor any agency thereof, nor any of their employees, makes any warranty, express or implied, or assumes any legal liability or responsibility, for the accuracy, completeness, or usefulness of any information, apparatus, product, or process disclosed, or represents that its use would not infringe privately owned rights. Reference herein to any specific commercial product, process, or service by trade name, trademark, manufacturer, or otherwise, does not necessarily constitute or imply its endorsement, recommendation, or favoring by the United States Government or any agency thereof. The views and opinions of authors expressed herein do not necessarily state or reflect those of the United States Government or any agency thereof.

ORNL/TM-11657
Dist. Category UC-202

Engineering Technology Division

TURBO REFRIGERATING COMPANY ICE STORAGE TEST REPORT

Therese K. Stovall

DATE PUBLISHED: June 1991

Prepared for
Electric Power Research Institute
under Interagency Agreement No. DOE ERD-85-502

Prepared by the
OAK RIDGE NATIONAL LABORATORY
Oak Ridge, Tennessee 37831-6285
managed by
MARTIN MARIETTA ENERGY SYSTEMS, INC.
for the
U.S. DEPARTMENT OF ENERGY
under Contract No. DE-AC05-084OR21400

MARTIN MARIETTA ENERGY SYSTEMS LIBRARIES

3 4456 0354992 5

CONTENTS

	Page
LIST OF FIGURES	v
LIST OF TABLES	vii
ABBREVIATIONS AND SYMBOLS	ix
ACKNOWLEDGMENTS	xi
ABSTRACT	1
1. INTRODUCTION	1
2. SYSTEM DESCRIPTION	4
2.1 TURBO STORAGE SYSTEM	4
2.2 TEST FACILITY	5
3. SYSTEM TESTS	9
4. ANALYSIS METHODOLOGY	16
4.1 DATA PROCESSING	16
4.2 REFRIGERATION EFFECT	16
4.3 DISCHARGE ENERGY AVAILABLE	21
4.4 SHELL HEAT GAINS	22
5. RESULTS	23
5.1 CHARGING PERFORMANCE	23
5.2 DISCHARGE PERFORMANCE	35
5.3 STANDBY HEAT GAINS	38
5.4 POWER CONSUMPTION	38
6. CONCLUSIONS AND RECOMMENDATIONS	47
REFERENCES	48
APPENDIX: ISTF INSTRUMENTATION	49

LIST OF FIGURES

Figure		Page
1	ISTF configuration for Turbo dynamic ice harvester system tests, refrigerant-side components	5
2	ISTF configuration for Turbo dynamic ice harvester system tests, water-side components	6
3	Comparison of calculated refrigeration capacity for three different evaporator outlet flow estimation bases, compared with measured reduction in tank water temperature during cooldown test (0408)	18
4	Comparison of calculated refrigeration capacity for three different evaporator outlet flow estimation bases, compared with measured ice production during ice-making test (0513)	19
5	Comparison of heat injection measured on refrigerant and water sides of condenser during ice-making test (0513)	24
6	Condensing, evaporating, suction, and water temperature during cool-down cycle under manufacturer's recommended operating conditions (test 1001.003)	25
7	Condensing, evaporating, suction, and water temperatures during ice-making cycle under manufacturer's recommended operating conditions (test 1002.002)	26
8	Evaporating temperature during cooldown and ice-making cycles	27
9	Capacity of Turbo system under manufacturer's recommended operating conditions (tests 1001.003 and 1002.002)	28
10	Normalized capacity of Turbo system while making ice under manufacturer's recommended operating conditions (test 1002.002)	29
11	System capacity measured during ice-making tests for varying condensing temperatures and defrost schedules with compressor speed of 1550 rpm and original thermal expansion valves	30
12	Relationship between system capacity, condensing temperature, and defrost schedules for compressor speed of 1780 rpm with properly adjusted expansion valves	32
13	Ice production in four evaporator sections during test at 35-s defrost cycle time and 225-s ice-making cycle time at condensing temperature of 90°F	33

14 Comparison of three different methods of measuring discharge capacity 35

15 Cumulative discharge energy during discharge tests 0805 and 0924 36

16 Temperature of water leaving Turbo tank during two discharge tests 37

17 Compressor power consumption during cooldown and while making ice at manufacturer's recommended operating conditions (tests 1001.003 and 1002.002) 40

18 Total power consumption during ice making for varying condensing temperatures and defrost schedules with compressor speed of 1550 rpm and original thermal expansion valves 41

19 Compressor power consumption during ice making for varying condensing temperatures and defrost schedules with compressor speed of 1550 rpm and original thermal expansion valves 42

20 Relationship between total power consumption, condensing temperature, and defrost schedules for 1780-rpm compressor speed with properly adjusted expansion valves 44

21 Relationship between compressor power consumption, condensing temperature, and defrost schedules for 1780-rpm compressor speed with properly adjusted expansion valves 45

22 Compressor power use while chilling water 46

LIST OF TABLES

Table		Page
1	ISTF monitoring points for the Turbo system tests	7
2	Charge test sequence: dynamic ice builders	10
3	Planned discharge test sequence	10
4	Planned standby test sequence	10
5	Turbo charge tests	11
6	Turbo discharge tests	13
7	Variable definitions for multivariate regression analysis of ice-making performance	31
8	Variable coefficients and standard errors for multivariate regression analysis of ice-making performance	31
9	Variable coefficients and standard errors for multivariate regression analysis of power consumption during ice making	43

ABBREVIATIONS AND SYMBOLS

ARI	Air-Conditioning and Refrigeration Institute
c_p	liquid refrigerant specific heat, Btu/lb-°F
FE1	liquid refrigerant flow to the evaporator, lb
FE2	hot gaseous refrigerant flow to the evaporator, lb
FE6	water flow to the condenser, ft^3
H_1	refrigerant enthalpy entering the condenser, Btu/lb
H_2	refrigerant enthalpy before the thermal expansion valve, Btu/lb
H_{sat2}	saturated liquid enthalpy corresponding to the measured pressure, PE2, Btu/lb
H_5	refrigerant enthalpy at the evaporator outlet, Btu/lb
H_{10}	refrigerant enthalpy at the compressor suction, Btu/lb
Inew	0 for original expansion valves, 1 for new valves
ISTF	Ice Storage Test Facility
PC_c	power consumption, compressor only, kW/ton
PC_t	Power consumption, compressor only, kW/ton
P_D	compressor discharge pressure, psia,
pvc	polyvinyl chloride
$\dot{Q}_f$	heat rejected by the refrigerant in the condenser
$\dot{Q}_w$	heat absorbed by the cooling water
Re^*	refrigerating capacity predicted by the regression model, ton
Re_c	refrigeration capacity predicted by the compressor capacity curves, ton
Re_N	net refrigeration effect during any given time period, Btu
Re_r	refrigeration effect (or heat absorbed by refrigerant) at evaporator plates during a 6-s period, Btu
RPM	compressor speed, rpm
RTD	resistance temperature detector
SAS	programming language and statistical analysis program
SCR	semiconductor controlled rectifier
Shell	shell heat gains, Btu
Speed	0 for compressor speed of 1550 rpm, 1 for 1775 rpm
T_d	saturated discharge temperature, °F
t_D	time in defrost cycle for each plate, s
t_I	time in ice-making cycle for each plate, s
TE2	liquid refrigerant temperature at the outlet of the liquid suction heat exchanger, °F
TE19	water temperature exiting the condenser
TE20	water temperature into the condenser
T-h	ton-hour
T_s	saturated suction temperature, °F
T_{sat2}	saturation temperature corresponding to the measured pressure PE2, °F
$\dot{W}_c$	compressor power predicted by the manufacturer's data, bhp
W_p	circulating pump energy, Btu
ρ	density of water, lb/ft^3
τ_D	fraction of total time in defrost cycle $[\tau_D = 100 \times t_D/(t_D + t_I)]$, %

ACKNOWLEDGMENTS

This important research has been made possible by the support of the Electric Power Research Institute. I would like to thank the program manager, Ronald Wendland, for his critical support and enthusiasm. Turbo Refrigerating Company provided the first unit to be tested at the Ice Storage Test Facility. John Tomlinson of Oak Ridge National Laboratory designed the Ice Storage Test Facility, supervised its construction, and has provided valuable guidance during the testing process. Delmar Fraysier is the chief operator of the test facility and has made important contributions to the test procedures.

TURBO REFRIGERATING COMPANY ICE STORAGE TEST REPORT

Therese K. Stovall

ABSTRACT

The Ice Storage Test Facility (ISTF) is designed to test commercial ice storage systems. Turbo Refrigerating Company provided a storage tank and refrigeration system to make and harvest ice. The Turbo ice storage system was tested over a wide range of operating conditions. System performance was satisfactory under both charging and discharging conditions. The storage capacity closely matched the manufacturer's literature. Power consumption was greater than that quoted by the manufacturer. Based on experimental data, algorithms were derived to predict performance, both charging rate and power consumption, as a function of several operational parameters. Two discharge tests showed that the ice stored was nearly 100% available under reasonable discharge conditions. Companion reports describe ISTF test procedures and ice-making efficiency test results that are common to many of the units tested.

1. INTRODUCTION

Commercial air conditioning loads are a large component of the afternoon peak loads served by electric utilities. Increased use of cool storage would shift this electrical load from peak to off-peak periods. This shift would permit utilities to defer construction of additional generating capacity and reduce customers demand charges.

Although the number of cool storage installations in commercial buildings is growing, it represents only a small fraction of the potential market. One major barrier to the use of cool storage equipment has been uncertainties associated with the performance of this equipment. Uniform testing by an independent agency has not been available. The performance data available from manufacturers are varied in scope and detail from one type of device to another and across manufacturers as well. Often system performance values are given for only one operating point, making it difficult to predict performance under other operating conditions.

Electric Power Research Institute (EPRI) therefore sponsored the development of an Ice Storage Test Facility (ISTF) to permit uniform testing of commercial-size cool storage equipment of many different types and has initiated a detailed laboratory testing program. This testing serves two purposes: (1) it will provide uniform performance test results, and (2) it will promote system improvements based on experimental data. Uniform test results will be useful to utilities in promoting cool storage installation and use, to utilities in

requesting rate schedules from Public Utility Commissions, and to building designers in specifying appropriate equipment for their applications. The experimental data will also be useful to equipment designers because they will describe component behavior as well as overall system performance. Toward these ends, the ISTF was designed with the capability to test several types of ice makers. Real-time data acquisition and precise computer controls were included.

The ISTF can be used to test dynamic, liquid recirculation, secondary fluid, and direct expansion (DX) ice makers. The simplest ice maker is a DX machine. In a DX ice maker, the refrigerant is sent as a cold liquid into coils submerged in a tank of water. As the refrigerant passes through these coils, it absorbs heat from the water and evaporates. As the refrigerant leaves the coils, it is completely gaseous and usually slightly superheated. The water in the tank is thereby chilled until it becomes frozen. When the stored cooling is needed, the ice is melted by circulating warm water from the heat load through the ice tank and returning the chilled water to the heat load. This arrangement is called an exterior melt because the ice tube is melted from the outside.

In a secondary fluid system, the cold liquid refrigerant is sent to a heat exchanger outside the tank of water. A secondary fluid, typically a glycol mixture, is chilled in this heat exchanger. This secondary fluid is then sent to the tank of water where it absorbs heat from the water, again freezing the water in the tank. The secondary fluid can also be used to transfer the stored cooling to the heat load. This arrangement is called an internal melt. The stored cooling energy can also be transferred to the heat load by using an external melt as described for the DX system.

A liquid recirculation system is similar to the DX system because cold refrigerant is sent to coils submerged in the tank of water. However, in the liquid recirculation system, the amount of refrigerant circulated through the coils is typically two to three times greater than in a DX system so that only a portion of the refrigerant is evaporated and the coils remain full of liquid throughout their length. This additional refrigerant circulation is accomplished through the use of gravity feed or a refrigerant pump. The stored cooling energy is transferred to the heat load using an external melt arrangement.

A dynamic ice maker freezes ice using either a DX or a liquid overfeed arrangement. However, in a dynamic system, the ice is harvested on a periodic basis. This harvesting cycle reduces the ice thickness on the heat transfer surface of the chiller. After the ice is

harvested, it is stored in a slush or slurry of ice and water. The water is circulated to provide the stored cooling to the heat load.

This report describes the test results for the first unit tested in this facility, a dynamic ice maker furnished by the Turbo Refrigerating Company (Turbo) in 1987. The storage system and test facility are described fully in Chap. 2. Chapter 3 describes the tests that were performed to characterize the storage system, and Chap. 4 describes the analysis methods used to evaluate the performance data. The test results are discussed in Chap. 5, and recommendations are summarized in Chap. 6. Companion reports describe ISTF test procedures and ice-making efficiency test results that are common to many of the units tested.[1,2]

2. SYSTEM DESCRIPTION

2.1 TURBO STORAGE SYSTEM

The Turbo unit, model HP300-ASC, includes a compressor, ice storage tank, liquid suction heat exchanger, and four evaporator sections, each consisting of nine vertical plates. The Turbo model HP300-A is rated at 26.1 tons with 32°F water to the plates and a condensing temperature of 95°F (Ref. 3). The storage tank was designed to hold 212 ton-h worth of ice. This unit was equipped with a 40-hp belt-driven compressor so that the effect of varying the compressor speed could be measured. Turbo units are usually equipped with direct-driven compressor-motor sets. The ISTF condenser was used for heat rejection.

A dynamic ice-maker functions by freezing water in thin layers on evaporator plates and then periodically switching into a defrost mode to release these layers of ice from the ice-making surface and drop them into a storage tank. The Turbo system consists of a series of vertical hollow plates suspended over a large holding tank. Cold liquid refrigerant (CFC-22) is circulated inside the plates. As the refrigerant evaporates, it removes heat from the water flowing downward over the outside of the plates. Thermal expansion valves control the flow of refrigerant based on the temperature sensed at the outlet of each plate. Figures 1 and 2 show the instrumentation locations for the refrigerant and water sides, respectively, of the system. The Turbo unit uses a timed defrost cycle to temporarily heat the vertical plates (after ~0.25 in. of ice has built up on both sides of each plate), causing the ice adhering to these plates to drop into the storage tank. During each defrost cycle, a control valve closes off the liquid flow of refrigerant to the evaporator sections (only two of which are shown in Fig. 1). At the same time that this control valve is closed, the three-way valve located at the exit of *one* evaporator section changes position so that hot gas from the compressor outlet is admitted into that evaporator section. As this hot gas melts a small layer of ice next to the plate, the ice is released, and the hot gas is cooled and condensed to a liquid form. This liquid refrigerant then flows through the other three evaporator sections where it is again vaporized before returning to the compressor suction via the liquid suction heat exchanger. Each plate is typically defrosted once every 20 min. Because there are four sections of plates, the system therefore went through a defrost cycle about once every 5 min.

The Turbo ice tank was discharged by circulating the water in the tank through an external heat load, simulated by a simple electric heater in the test facility. A water distribution header above the vertical plates on the Turbo unit helps to provide adequate

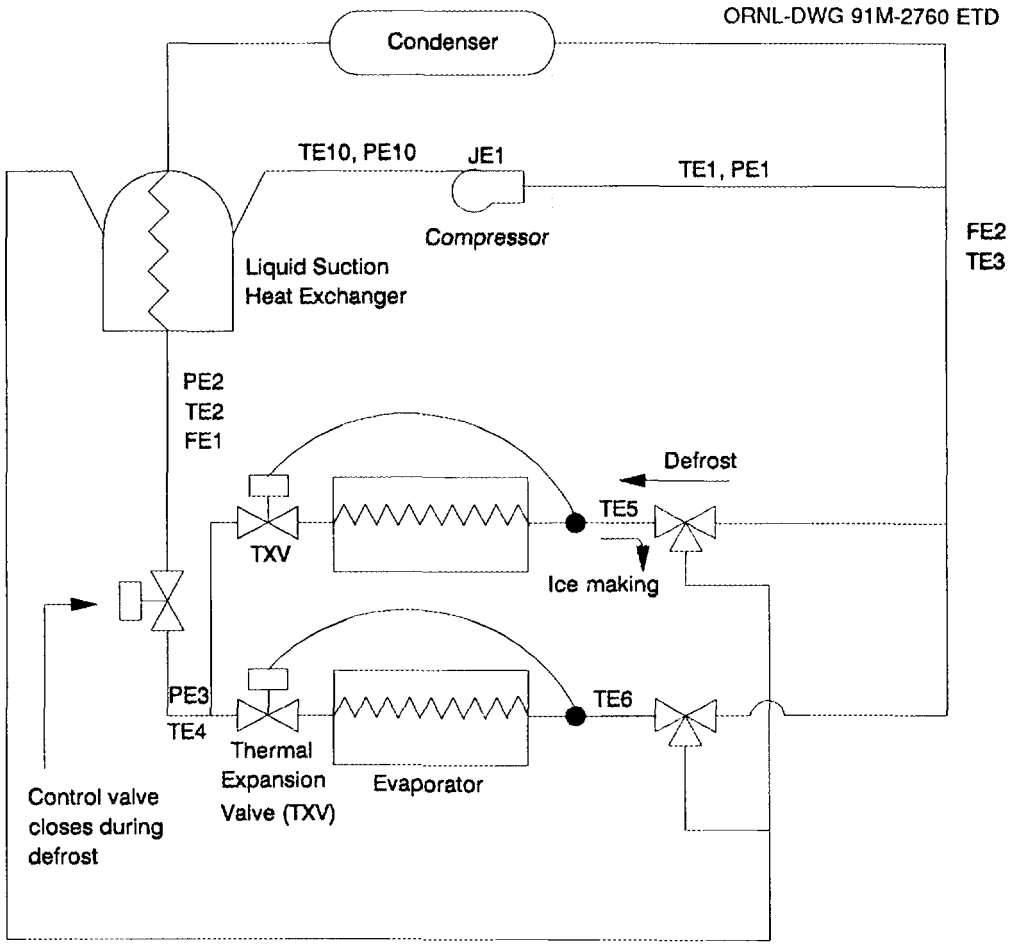

Fig. 1. ISTF configuration for Turbo dynamic ice harvester system tests, refrigerant-side components.

water mixing during the discharge cycle and in the chilling portion of any charging cycle. It is important not to freeze the tank fully solid but to leave enough free water to ensure adequate water circulation passages within the ice tank. The ice tank is equipped with an ice inventory sensor to avoid overcharging the tank. This sensor is not designed to provide information during a discharge cycle or to measure the state of charge at any level less than fully charged. The Turbo tank was filled with the recommended volume of 3400 gal for most tests.

2.2 TEST FACILITY

The test facility was designed to test a wide variety of storage systems. It includes all refrigeration system components necessary to test dynamic, liquid overfeed, and brine systems.

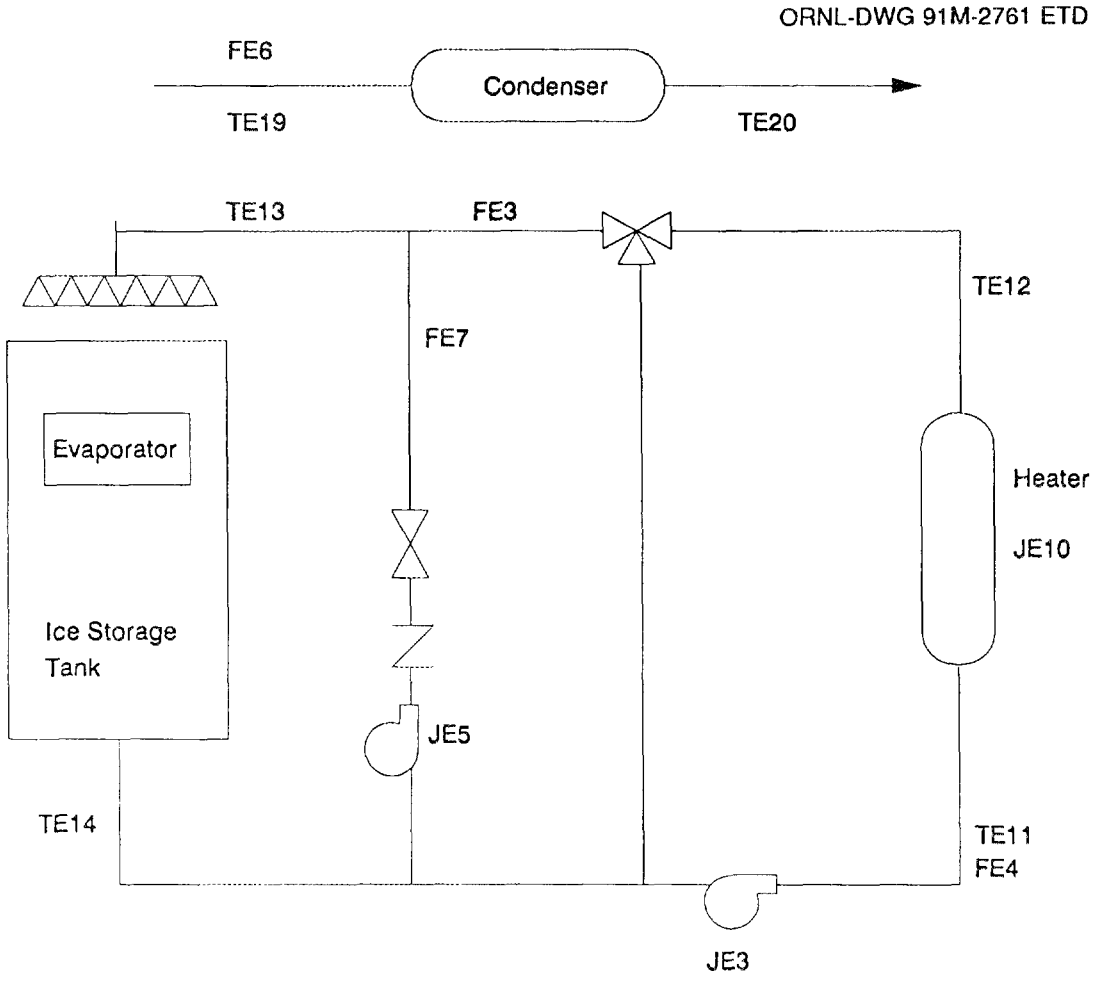

Fig. 2. ISTF configurations for Turbo dynamic ice harvester system tests, water-side components.

The Turbo system was a unitary model requiring only the use of the ISTF condensers for heat rejection and the ISTF load simulator for discharge. The 40-ton condenser was used for these tests, and the condensing temperature was controlled by varying the flow of the cooling water to the condenser. The load simulator consists of an electric resistance heater with a variable power supply and a maximum rating of 135 kW, a variable speed pump, and a booster pump. A three-way valve arrangement at the heater outlet can divert a portion of the heater outlet flow to the pump inlet. This permits exact control of the heater inlet temperature.

Modifications were made by Turbo to the unit to accommodate the monitoring points, such as flowmeters, necessary to assess the system performance. The test facility is well-

equipped with monitoring devices to measure temperature, pressure, flow, and energy use. The monitoring points shown in Figs. 1 and 2 are listed in Table 1. The test loop instrumentation is described more fully in the Appendix and Ref. 1.

Refrigerant temperature measurements were made by resistance temperature detectors (RTDs) bonded to the outside of the copper lines, and therefore they imposed no

Table 1. ISTF monitoring points for the Turbo system tests

Point label	Measured quantity
FE1	Liquid refrigerant flow to the evaporator
FE2	Hot gaseous refrigerant flow to the evaporator
FE3	Ice tank inlet flow, water
FE4	Heater inlet flow, water
FE6	Condenser inlet flow, water
FE7	Ice tank inlet flow, water
JE1	Compressor energy and power
JE3	Water pump energy and power
JE5	Circulation pump energy and power
JE10	Heater energy and power
PE1	Compressor discharge pressure
PE2	Refrigerant pressure at the liquid suction heat exchanger liquid-side outlet
PE3	Refrigerant pressure to the thermal expansion valves
PE10	Compressor suction pressure
TE1	Compressor discharge temperature
TE2	Refrigerant temperature at the liquid suction heat exchanger liquid-side outlet
TE3	Hot defrost gas temperature
FE4	Refrigerant temperature before the thermal expansion valves
TE5/TE6	Evaporation section outlet (during ice making)/ inlet (during defrost) temperature
TE9	Heat exchanger inlet temperature
TE10	Compressor suction temperature
TE11	Heater inlet water temperature
TE12	Heater outlet water temperature
TE13	Ice tank inlet water temperature
TE14	Ice tank outlet water temperature
TE19	Condenser inlet water temperature
TE20	Condenser outlet water temperature

flow restrictions on the refrigeration system. Flow measurements, however, involve additional piping and flowmeters that caused system pressure drops. The flowmeter used to measure the liquid refrigerant flow to the evaporator caused a pressure drop of ~0.45 psi. The additional piping, including fittings and valves, caused another drop of ~0.6 psi. Together, these pressure drops were equivalent to a temperature penalty of ~0.4°F (Refs. 4 and 5). Based on the compressor ratings, this caused a decrease in the compressor capacity of ~0.1 ton or ~0.4% decrease in capacity during the ice-making cycle.[6]

The pressure drop through the flowmeter used to measure the hot refrigerant gas flow for the defrost cycle was 5.6 psi, and the pressure drop due to the associated piping was 0.7 psi (Refs. 4 and 5). Together, these pressure drops caused a temperature penalty of ~2.2°F. Based on the compressor ratings, this caused a decrease in the compressor capacity of ~0.5 ton or ~2% decrease in capacity during the defrost cycle.[6]

3. SYSTEM TESTS

The test plan was structured to test the storage tank's capabilities over a wide range of operating conditions. The compressor speed and discharge pressure and the amount of time spent in the ice-making and defrost modes of operation were the controlled variables during the charging tests. The heater power and the water temperature entering and exiting the heater were the controlled variables during the discharge tests. Additional tests were made to measure the physical ice inventory as a check against the refrigeration effect calculated from the measured refrigerant flows, pressures, and temperatures.

The test schedule included efforts to characterize compressor performance as a function of saturated discharge and evaporating temperatures. The amount of ice made for varying ice-making/defrost schedules was also tested. The ice-discharge tests were designed to mimic different discharge periods ranging from 6 to 12 h with varying temperature and flow requirements at the heater. Tables 2–4, taken from the ISTF test procedure, show the desired testing schedule.[1] However, this procedure was in the process of revision during the Turbo tests. (Indeed, many revisions were prompted by the experience gained during the Turbo tests.) Since these tables are taken from a generic test procedure, they refer to a "manufacturer's recommended time" for both the overall cycle and the defrost period. For the Turbo unit, the recommended times were a 376-s chilling period followed by a 35-s defrost period. Tables 5 and 6 present a summary of the tests that were used to analyze the Turbo storage system performance.

Various combinations of the ice-making and defrost periods covered system performance under conditions where the defrost cycled ranged from 7 to 20% of the total cycle time. Turbo's recommended operating point is at ~8.5% defrost. Attempts to run tests at defrost times shorter than 7% were unsuccessful because of ice-bridging problems between the evaporator plates. Apparently, the recommended operating condition is closely tied to the machine's physical design, with an appropriate margin of safety.

For each combination of testing parameters, data were taken over at least four complete defrost cycles so that each of the four ice-making section's performance during the defrost cycle could be examined. Data were taken on 39 channels at 6-s intervals to allow complete analysis of the dynamics of the ice-making and defrost cycles.

The first, and most direct, method used to measure the ice-making performance was to catch the ice as it fell from the evaporator sections in a large net. This net was attached

Table 2. Charge test sequence: dynamic ice builders
(Defrost cycle time is as recommended by manufacturer)

Test No.	Saturated discharge temperature (°F)	Total cycle time (h)
1	105	MR[a]
2	95	MR
3	85	MR
4	105	0.5 × MR
5	95	0.5 × MR
6	85	0.5 × MR
7	105	2 × MR
8	95	2 × MR
9	85	2 × MR
10	105	1.5 × MR
11	95	1.5 × MR
12	85	1.5 × MR
13	105	MR
14	95	MR
15	85	MR

[a]Manufacturer's recommended cycle times. (The recommended cycle for this four-section unit was 376-s ice-making and 35-s defrost.)

Table 3. Planned discharge test sequence

Test No.	Test duration (h)	TE12 (°F)	TE11 (°F)
1	6	60	38
2	9	60	45
3	12	60	45
4	6	50	38
5	9	50	38
6	12	50	45

Table 4. Planned standby test sequence

Test No.	Test duration (h)	Initial tank condition
1	>60	Fully frozen
2	>60	Fully frozen

Table 5. Turbo charge tests

Month	Day	Test sequence No.	Chilling period (s)	Defrost period (s)	Discharge pressure (psia)	Test conditions	Compressor speed (rpm)
04	07	DAT	325	25	211	Cooldown	1550
04	08	DAT	325	25	211	Cooldown	1550
04	13	002	325	45	211	Ice making	1550
04	13	004	325	45	183	Ice making	1550
04	13	006	325	45	158	Ice making	1550
04	14	002	285	45	158	Ice making	1550
04	14	004	285	45	183	Ice making	1550
04	14	006	285	45	211	Ice making	1550
04	15	006	285	35	158	Ice making	1550
04	15	004	285	35	183	Ice making	1550
04	15	002	285	35	211	Ice making	1550
04	20	003	225	25	211	Ice making	1550
04	20	002	225	25	183	Ice making	1550
04	20	001	225	25	158	Ice making	1550
04	21	002	285	25	183	Ice making	1550
04	21	001	285	25	211	Ice making	1550
04	22	006	225	45	158	Ice making	1550
04	22	005	225	45	183	Ice making	1550
04	22	004	225	45	211	Ice making	1550
04	22	003	225	35	211	Ice making	1550
04	22	002	225	35	183	Ice making	1550
04	22	001	225	35	158	Ice making	1550
04	23	002	165	45	183	Ice making	1550
04	23	001	165	45	158	Ice making	1550
04	24	001	165	45	211	Ice making	1550
04	24	002	165	35	211	Ice making	1550
04	24	003	165	35	183	Ice making	1550
04	24	004	165	35	158	Ice making	1550
04	24	005	165	25	158	Ice making	1550
04	24	006	165	25	183	Ice making	1550
04	24	007	165	25	211	Ice making	1550
04	27	001	325	45	211	Ice making	1550
04	27	002	325	45	183	Ice making	1550
04	28	001	325	45	158	Ice making	1550
04	28	002	325	25	158	Ice making	1550
04	28	003	325	25	211	Ice making	1550
04	29	001	325	25	183	Ice making	1550

Table 5 (continued)

Month	Day	Test sequence No.	Chilling period (s)	Defrost period (s)	Discharge pressure (psia)	Test conditions	Compressor speed (rpm)
05	06	007	325	25	183	Ice making	1550
05	06	005	325	25	211	Ice making	1550
05	13	001	325	35	183	Cooldown	1550
05	13	002	325	35	183	Continuation	1550
05	13	003	325	35	183	Continuation	1550
05	13	004	325	35	183	Continuation	1550
05	13	005	325	35	183	Continuation	1550
05	13	006	325	35	183	Ice making	1550
05	13	007	325	35	183	Continuation	1550
05	13	008	325	35	183	Continuation	1550
05	19	001	325	35	183	Cooldown	1550
06	23	001	325	35	183	Cooldown	1775
06	23	003	325	35	183	Ice making	1775
06	24	001	325	35	211	Ice making	1775
06	24	002	325	45	211	Ice making	1775
06	24	003	325	45	183	Ice making	1775
06	24	004	325	45	158	Ice making	1775
06	30	002	325	35	183	Ice making	1775
06	30	003	325	35	183	Continuation	1775
06	30	004	325	35	183	Continuation	1775
06	30	005	325	35	183	Continuation	1775
06	30	006	325	35	183	Continuation	1775
06	30	007	325	35	183	Continuation	1775
06	30	008	325	35	183	Continuation	1775
06	30	009	325	35	183	Continuation	1775
06	30	001	325	35	183	Cooldown	1775
07	01	001	310	35	197	Ice making	1775
07	01	002	310	35	197	Continuation	1775
07	07	002	325	35	197	Ice making	1775
07	07	003	325	45	197	Ice making	1775
07	09	001	325	25	211	Cooldown	1775
07	09	002	325	25	211	Cooldown	1775
07	09	003	325	25	211	Cooldown	1775
08	03	001	325	35	183	Cooldown	1775
08	03	002	325	35	183	Continuation	1775
08	03	003	325	35	183	Continuation	1775
08	03	004	325	35	183	Ice making	1775
08	03	005	325	35	183	Continuation	1775
08	04	001	325	35	183	Continuation	1775
08	04	002	325	35	183	Continuation	1775
08	04	003	325	35	183	Continuation	1775

Table 5 (continued)

Month	Day	Test sequence No.	Chilling period (s)	Defrost period (s)	Discharge pressure (psia)	Test conditions	Compressor speed (rpm)
08	26	001	325	35	183	Ice making	1775
08	26	002	325	35	183	Continuation	1775
08	26	003	325	35	158	Ice making	1775
08	31	001	325	35	183	Cooldown	1775
09	22	001	325	35	183	Cooldown	1775
09	22	002	325	35	183	Ice making	1775
09	22	003	325	35	183	Continuation	1775
09	22	004	325	35	183	Continuation	1775
09	23	001	325	35	183	Continuation	1775
09	23	002	325	35	183	Continuation	1775
09	23	003	325	35	183	Continuation, freeze-up	1775
09	30	001	376	35	183	New valves	1775
09	30	002	376	35	197	New valves	1775
10	01	001	376	35	183	New valves	1775
10	01	002	376	35	197	New valves	1775
10	01	003	376	35	197	Cooldown	1775
10	02	001	376	35	197	New valves	1775
10	02	002	376	35	197	New valves	1775
10	02	003	376	35	197	New valves	1775
10	02	004	376	35	197	New valves	1775
10	05	001	325	35	197	New valves	1775
10	05	002	325	35	211	New valves	1775
10	05	003	325	35	183	New valves	1775
10	06	001	325	45	183	New valves	1775
10	06	002	325	45	183	New valves	1775
10	06	003	285	45	183	New valves	1775
10	06	004	285	45	183	New valves	1775

Table 6. Turbo discharge tests

Test ID	Test duration (h)	Nominal heater power (kW)	Water flow rate (gal/min)
0805	7	100	90
0924	7.5	95	90

to a scale to measure directly the amount of ice produced by each section of plates in the given test period. Ambient infiltration will introduce a small amount of error to this approach. However, these heat gains should not be significant because the test facility is located in an indoor, sheltered location (i.e., no solar gains and no wind).

Following performance tests, the amount of ice in the tank was also measured by draining the remaining water in the tank through a flowmeter. This measurement of the water removed, along with the known quantity of water in the tank before the test began, gives an accurate measurement of the amount of ice made during the test. Some water will remain trapped in the ice during any such draining process. However, later continuous drainage tests (used for the standby loss test) showed that the amount of such trapping was relatively small compared with the large quantities under consideration during the performance testing.

The wide range of performance parameters tested spanned the operating points found in most commercial applications. This range of conditions tested the capability of the refrigerant expansion valves that are usually fine-tuned to a specific operating point to adjust the refrigerant flow with capacity. Because the operation of these valves is critical to the unit's performance, this issue was deemed important. The original valves were adjusted for an operating point near the middle of the anticipated testing conditions. After the majority of the tests were completed, the valves were replaced and carefully adjusted to Turbo's recommended operating conditions. Several additional tests were run with these new valves, both at the recommended operating point and also at operating points previously tested. This permitted an examination of a representative commercial installation and also provided an opportunity to quantify the potential improvements attainable with correct expansion valve adjustment.

The water flow was contained in uninsulated polyvinyl chloride (PVC) pipes. Because a small amount of condensation was visible on these pipes during tests, it was necessary to investigate the impact of heat gains through the pipe wall. This was checked in two ways. First, chilled water was circulated through a major portion of the piping and the temperature was measured at two thermocouple positions. This test showed no detectable rise in the water temperature. Second, that portion of the PVC piping used during the ice-making process was insulated, and several ice-making performance tests were repeated for comparison. No improvement in performance was measured.

The discharge performance was investigated to be certain that all of the energy stored would be available during discharge. Water was circulated from the storage tank to a heater used to simulate the building load. The physical behavior of the ice within the storage tank was visually observed, and the temperature of the water leaving the storage tank was recorded over the entire discharge cycle.

A biological ice nucleator additive was also tested.[7] The additive, called Snomax™, is typically used in snow machines to raise the temperature at which water changes to ice by acting as a catalyst to start ice crystal formation. It was tested with the Turbo system to determine if it would enhance the performance of the machine by both raising the evaporating temperature and by improving the transition from defrost to ice making. Two tests were made with the Snomax additive that duplicated tests made without the additive.

Tank heat gains were measured by recording the change in ice inventory over a long period of time in the absence of all external fluid flows and with the tank covers in place. The ice depletion over these time periods was ascribed to shell heat gains. The ice depletion was determined by (1) measuring the amount of water in the tank, (2) freezing a large portion of this water, (3) draining (and measuring) the remaining water in the tank, and then (4) recording the drainage rate vs time while the ice melted within the tank.

Other standby heat gain tests were conducted by measuring the temperature rise in a tank full of chilled water without any ice. For these tests, the water temperature was measured after a mixing period of at least 10 min, before and after a long period of time without any external fluid flows. The ambient temperature was also noted during all standby tests. However, the ambient conditions showed little variation because of the sheltered location of the test floor.

4. ANALYSIS METHODOLOGY

4.1 DATA PROCESSING

The data available for each test permit redundant calculations that increase our understanding and confidence in the test results. For example, the heat rejection at the condenser is measured on both the water and refrigerant sides of the heat exchanger. The refrigeration effect to the ice tank is measured by both changes in the ice inventory and by the refrigerant flow and enthalpy change across the evaporator. The energy available for discharge is measured by water flow and temperatures at the heater and at the ice tank, as well as by monitoring the power going to the discharge heater.

The data are collected for each monitoring point every 6 s during a charge test and every 30 s or 1 min during a discharge test. The collection frequency during the charge test is dictated by the dynamics of the ice-making/defrost cycle, where the defrost cycle can last from 20 to 30 s.

Thermodynamic properties for the refrigerant CFC-22 are calculated from a computerized format developed by G. T. Kartsounes and R. A. Erth and adapted for use at Oak Ridge National Laboratory (ORNL) by C. K. Rice and S. K. Fischer.[8]

Linear regression was used to correlate the various operating parameters to the measured ice-making capacity. A SAS system procedure entitled REG was used for this purpose.[9] This procedure fits least-squares estimates to linear regression models and reports the adjusted squared correlation coefficient as well as the Student's t-ratio and significance probability for each parameter estimate.

4.2 REFRIGERATION EFFECT

An energy balance on the refrigerant side of the evaporator was used to provide a continuous measure of the refrigeration effect throughout each charge test.

$$Re_r = FE1 \times H_2 + FE2 \times H_1 - (FE1 + FE3) \times H_5 , \qquad (1)$$

where

Re_r = refrigeration effect (or heat absorbed by refrigerant) at evaporator plates during a 6-s period (Btu),

FE1 = liquid refrigerant flow to the evaporator (lb),

H_2 = refrigerant enthalpy before the thermal expansion valve (Btu/lb),

FE2 = hot gaseous refrigerant flow to the evaporator (lb),

H_1 = refrigerant enthalpy corresponding to measured compressor discharge temperature and pressure (Btu/lb),

H_5 = refrigerant enthalpy at the evaporator outlet (Btu/lb).

Several assumptions are inherent in this equation: (1) adiabatic expansion at the thermal expansion valves, (2) steady-state, steady-flow conditions at the liquid suction heat exchanger, (3) the evaporator outlet pressure equal to the compressor suction pressure, and (4) the instantaneous evaporator outlet flow equal to the sum of the instantaneous evaporator inlet flows. The liquid and gaseous refrigerant flows to the evaporator sections are directly measured and recorded every 6 s. The refrigerant enthalpy before the thermal expansion valves is calculated based on the condensing pressure and the temperature at the outlet of the liquid suction heat exchanger.

$$H_2 = H_{sat2} - c_p \times (T_{sat2} - TE2) , \tag{2}$$

where

H_{sat2} = saturated liquid enthalpy corresponding to the measured pressure, PE2, (Btu/lb),

c_p = liquid refrigerant specific heat (Btu/lb-°F),

T_{sat2} = refrigerant saturation temperature corresponding to the measured pressure PE2 (°F),

TE2 = liquid refrigerant temperature at the outlet of the liquid suction heat exchanger (°F).

The refrigerant at the compressor outlet is superheated, and the enthalpy is directly available from the measured pressure and temperature at this point. The refrigerant at the evaporator outlet, H_5, is usually superheated and also directly available from the measured temperature and the compressor suction pressure. However, sometimes the refrigerant at the evaporator outlet is not superheated. When this occurs, usually during the defrost cycle, the evaporator outlet enthalpy is calculated from a balance on the liquid suction heat exchanger.

$$H_5 = H_2 - H_{sat2} + H_{10} , \tag{3}$$

where H_{10} is the refrigerant enthalpy at the compressor suction based on the measured pressure and temperature.

As noted previously, the evaporator outlet flow was assumed to equal the sum of the inlet flows. Two alternate methods of estimating this value were also investigated. The first

calculated the average refrigerant flow to the compressor over the entire test period and used this average as a constant value during the analysis. The second alternate method calculated the exit flow based on the compressor power consumption for each 6-s scan period and the compressor curves described later in this report. Over a 4-h test period, the base and first alternate assumptions produce the same estimate of total refrigeration to within 0.5% during ice making and 0.01% during cooldown. Portions of these tests are shown in Figs. 3 and 4. The assumption based on the compressor curves led to a refrigeration estimate that was ~10% higher during ice making and ~3% higher during cooldown than the other two (tests 0408 and 0513). The results based on the base and first alternate assumptions were closer to the results based on the water-side measurements (discussed below). Also, the assumption

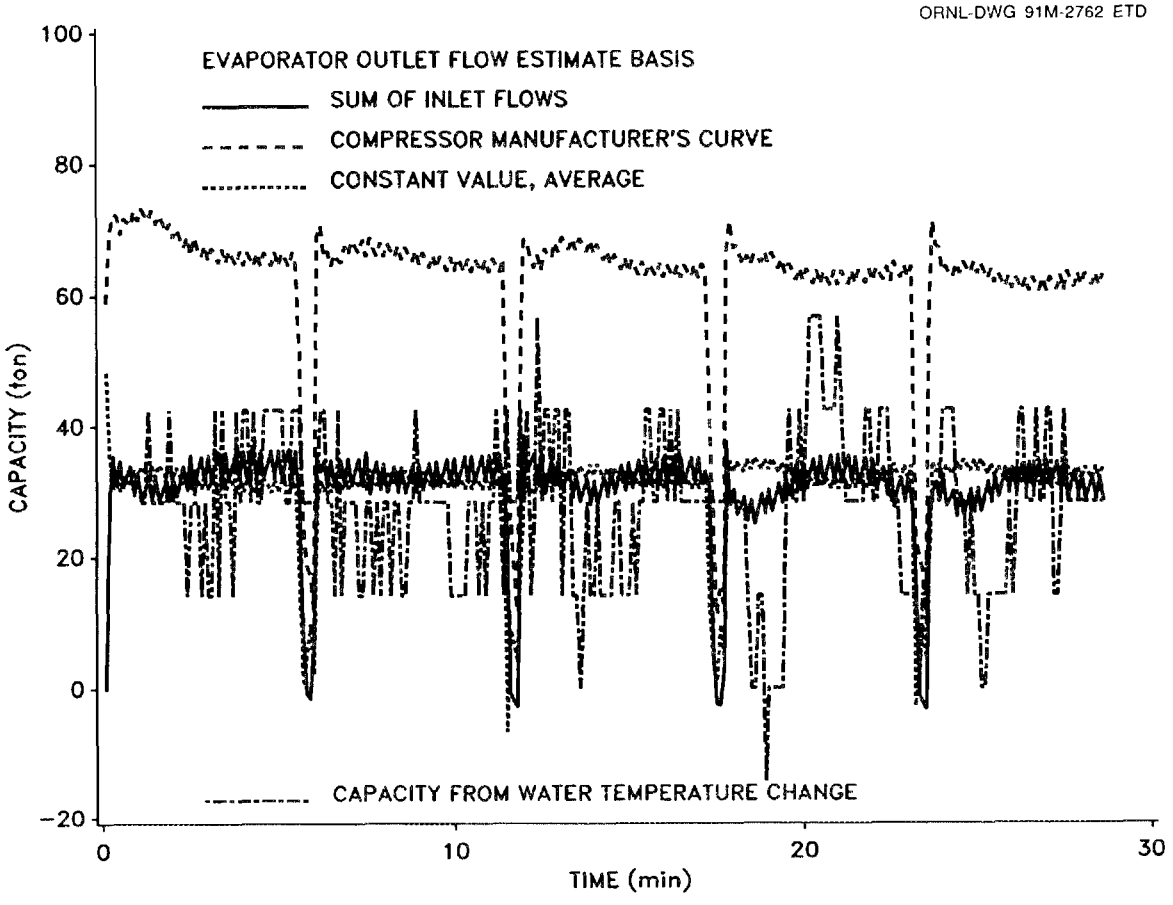

Fig. 3. Comparison of calculated refrigeration capacity for three different evaporator outlet flow estimation bases, compared with measured reduction in tank water temperature during cooldown test (0408).

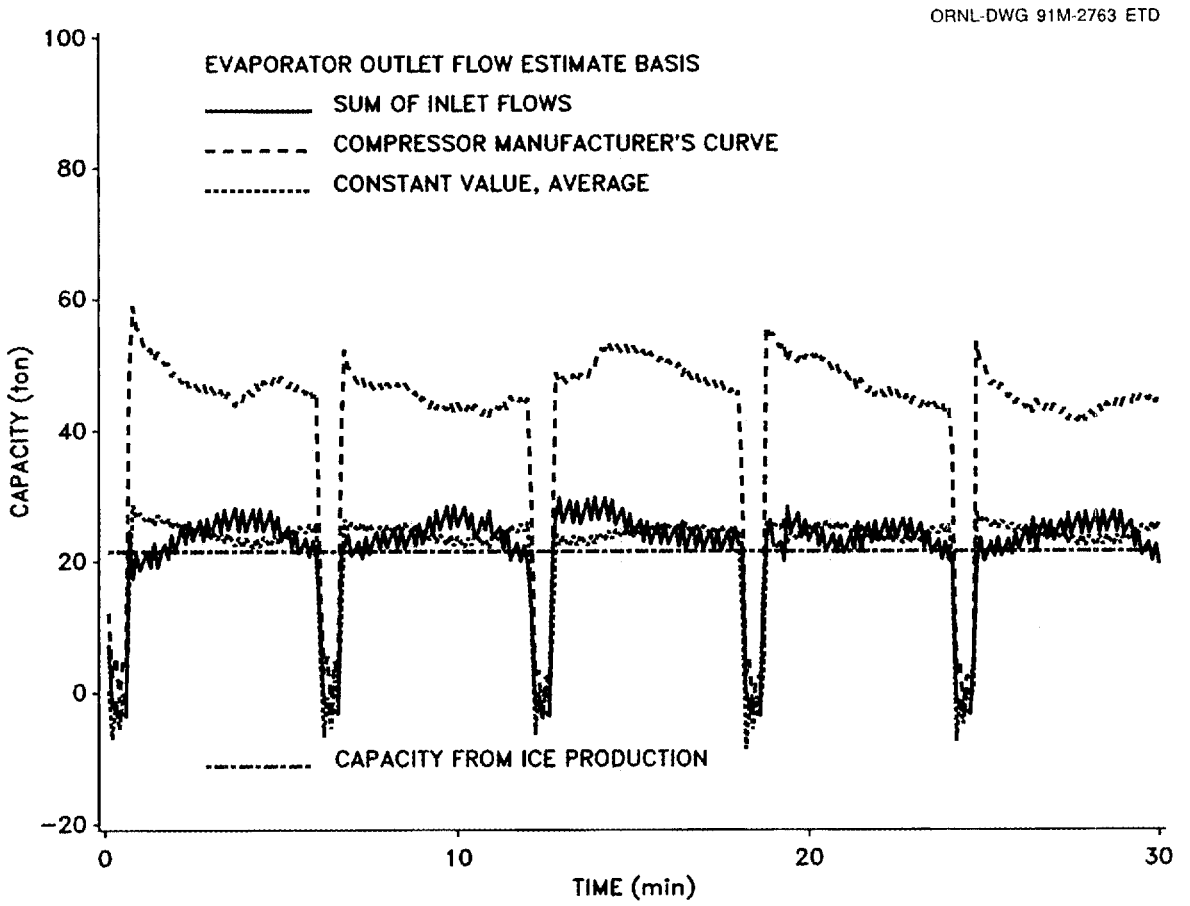

Fig. 4. Comparison of calculated refrigeration capacity for three different evaporator outlet flow estimation bases, compared with measured ice production during ice-making test (0513).

that the evaporator exit flow was equal to the inlet flow was the most closely related to the actual data. This first assumption was therefore used for all subsequent analyses.

The water-side measurements reflect only the useable chilling capacity. The useable chilling capacity is the evaporator capacity less the amount of energy added to the water by the circulating pump and the amount of energy absorbed into the storage structure shell from the surroundings.

$$Re_N = Re_r - W_p - \text{Shell} , \tag{4}$$

where

Re_N = net refrigeration effect during any given time period (Btu),

W_p = circulating pump energy (Btu),

Shell = shell heat gains (Btu).

It was necessary to compare the chilling capacity [based on Eqs. (1) and (4)] to a more direct measurement to validate the assumptions previously discussed. Two separate tests were made for this purpose. The first test compared the measured heat absorbed by the refrigerant to the measured heat removed from the water as the water was cooled from 50 to 38°F (the machine was set to cycle through the defrost cycle during this test, although during normal operation and during all other tests the defrost cycles are not initiated until the water temperature falls below 38°F). The second test compared the heat absorbed by the refrigerant during a long test starting with a known quantity of water (with no ice) in the tank at ~38°F through ~6 h of ice making. At the end of that time, the water remaining in the tank was drained through a flowmeter to measure the amount of ice made during the charging period. The results of these tests are described more fully in Sect. 5.1 and tend to impart a high level of confidence (with an accuracy of ~5%) in the calculated values.

Another measurement of the system capacity can be taken from the compressor curves provided by the manufacturer. These curves were modeled as

$$\begin{aligned} Re_c = {} & 49.35 + 1.663 \times T_s - 0.00173 \times (T_d)^2 \\ & - 0.00708 \times T_s \times T_d + 0.00953 \times (T_s)^2 , \end{aligned} \tag{5}$$

$$\begin{aligned} W_c = {} & 44.088 - 0.508 \times T_s + 0.000840 \times (T_d)^2 \\ & + 0.0123 \times T_s \times T_d - 0.00592 \times (T_s)^2 , \end{aligned} \tag{6}$$

$$\dot{Q}_c = 1.090 - 0.00422 \times T_s + 0.00263 \times T_d , \tag{7}$$

where

Re_c = refrigeration capacity predicted by the compressor capacity curves (ton),

T_s = saturated suction temperature (°F),

T_d = saturated discharge temperature (°F),

$\dot{W}_c$ = compressor power predicted by the manufacturer's data (bhp),

$\dot{Q}_c$ = heat of rejection predicted by the compressor manufacturer (ton).

Equation (5) predictions match the compressor manufacturer's table within ±0.5 ton. Equation (6) predictions match the manufacturer's table within ±0.5 hp. The heat of rejection model, Eq. (7), has residuals ranging from −0.005 to +0.016.

As another check on the system, the heat rejected at the condenser is measured on both the refrigerant and water sides as:

$$Q_w = FE6 \times (TE20 - TE19) \times c_p \times \rho \,, \tag{8}$$

$$Q_f = (FE1 + FE2) \times (H1 - H_{SAT2}) \,, \tag{9}$$

where

Q_w = heat absorbed by the cooling water (Btu),
FE6 = water flow (ft^3),
TE20 = water temperature into the condenser (°F),
TE19 = water temperature exiting the condenser (°F),
Q_f = heat rejected by the refrigerant (Btu),
H_1 = refrigerant enthalpy entering the condenser (Btu/lb),
H_{SAT2} = refrigerant enthalpy leaving the condenser (Btu/lb),
c_p = specific heat of water (Btu/lb-°F),
ρ = density of water (lb/ft^3).

A normalized capacity is also calculated to provide a clearer picture of the change in capacity during the charging cycle. The normalized capacity is equal to the capacity at each point in time divided by the average capacity over the entire charging test period.

4.3 DISCHARGE ENERGY AVAILABLE

The cool storage available to meet a cooling load was measured by the water flow rates and temperature changes at the heater and at the ice tank.

$$cap_h = FE4 \times (TE12 - TE11) \times c_p \times \rho \,, \tag{10}$$

$$cap_t = FE3 \times (TE13 - TE14) \times c_p \times \rho \,, \tag{11}$$

where

cap_h = discharge capacity measured at the heater (Btu),
FE4 = water flow to heater (ft^3),
TE12 = water temperature leaving heater (°F),
TE1 = water temperature entering heater (°F),
cap_t = discharge capacity measured at the ice tank (Btu),
FE3 = water flow to ice tank (ft^3),

TE13 = water temperature to ice tank (°F),

TE14 = water temperature leaving ice tank (°F).

The heater power was also measured but is not considered accurate as is discussed in the Appendix. The tank was considered to be fully discharged when the tank outlet temperature reached 44°F. Some ice may remain in the tank at that time, but it is unavailable to meet the load.

4.4 SHELL HEAT GAINS

Shell heat gains were measured directly from changes in tank water temperature and ice inventory over extended periods of time when there was no external flow.

5. RESULTS

5.1 CHARGING PERFORMANCE

As described in Sect. 4.2, two tests were made to evaluate the accuracy of the calculations used to measure the cooling effect based on refrigerant measurements. In these two tests, 0408 and 0513, carefully controlled conditions on the water-side of the system enabled a direct comparison to the cooling effect as measured by the water and as measured by the refrigerant. During the cooldown comparison (test 0408), the refrigeration effect based on refrigerant measurements was 9% larger than that based on the water measurements (Fig. 3). During the ice-making test (test 0513), performance estimates based on the refrigerant measurements predicted 7% more ice than was measured as is shown in Fig 4. Most of these differences between the water measurements and the refrigerant measurements can be explained by including the effect of tank jacket losses ($\sim$0.4 ton or $\sim$2%) and the energy input of the water circulating pump ($\sim$0.6 ton or $\sim$3%) as shown previously in Eq. (4). The remaining difference of $\sim$2 to 4% is likely attributable to the limitations of instrumentation accuracy given in the Appendix.

A similar comparison of the heat of rejection measurements at the condenser was made for test 0513 (Fig. 5). This condenser balance showed 9% more heat removed from the refrigerant than was absorbed by the water. Thermal losses from the condenser shell were unaccounted for but were deemed to be small because the ambient temperature was very near the average shell water temperature. The remainder of the difference is likely attributable to instrument accuracy limitations.

When charging a dynamic ice-maker storage tank, the compressor suction temperature gradually drops as the water in the tank becomes colder. The reduced suction temperature leads to a reduced refrigeration capacity. Once ice begins to build on the plates, the compressor begins to cycle through a series of ice-making and defrost periods. The suction temperature reaches its lowest value just before a defrost cycle begins. Therefore, the performance of the system can be represented by the performance during the shortest period of time necessary for each section of plates to go through the ice-making and defrost cycles. This is unlike other ice storage systems where performance characterizations require tests that go from the fully melted to the fully frozen state, because the charging capacity of a dynamic chiller, unlike other ice storage systems, is not a function of the tank state of charge.

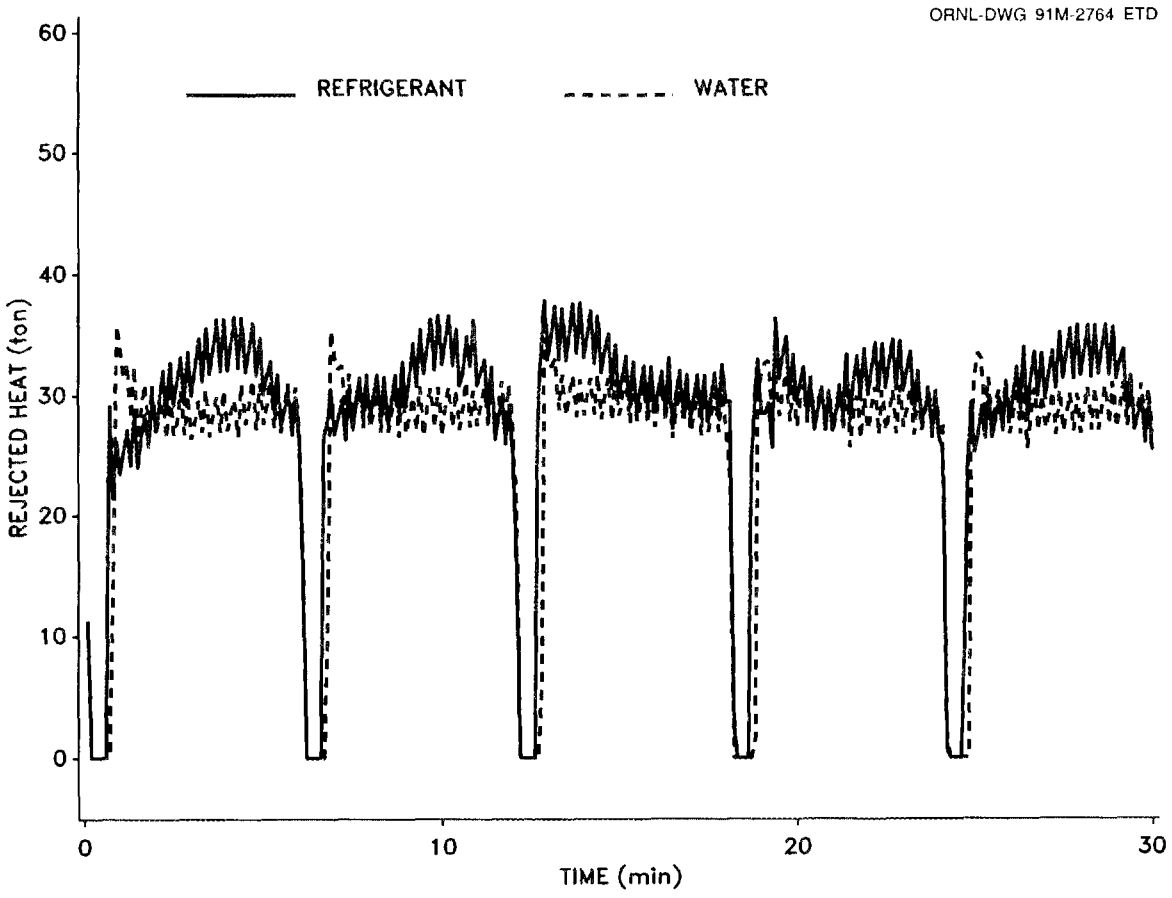

Fig. 5. Comparison of heat injection measured on refrigerant and water sides of condenser during ice-making test (0513).

The Turbo unit was tested at conditions recommended by the manufacturer with a saturated discharge temperature of 95°F, a defrost cycle time of 35 s, and an ice-making time of 375 s (corresponding to an overall cycle time for all four plates of 1640 s). Figures 6 and 7 show the relationships between the condensing temperature, the refrigerant temperature leaving the evaporator, the water temperature, and the evaporating temperature during an extended test at these conditions (tests 1001.003 and 1002.002). Figure 6 shows the system temperatures during the cooldown portion of the cycle (i.e., before ice-making and defrost cycles begin). The suction temperature shows some mild variations but is relatively well controlled with a superheat ranging from 2 to 10°F. Figure 7 shows these same temperatures while the system is making ice. The defrost cycles are readily apparent from the condensing temperature, which tends to drop ~10°F during the defrost cycle. The suction temperature is relatively flat with very little superheat. A direct comparison of the evaporating

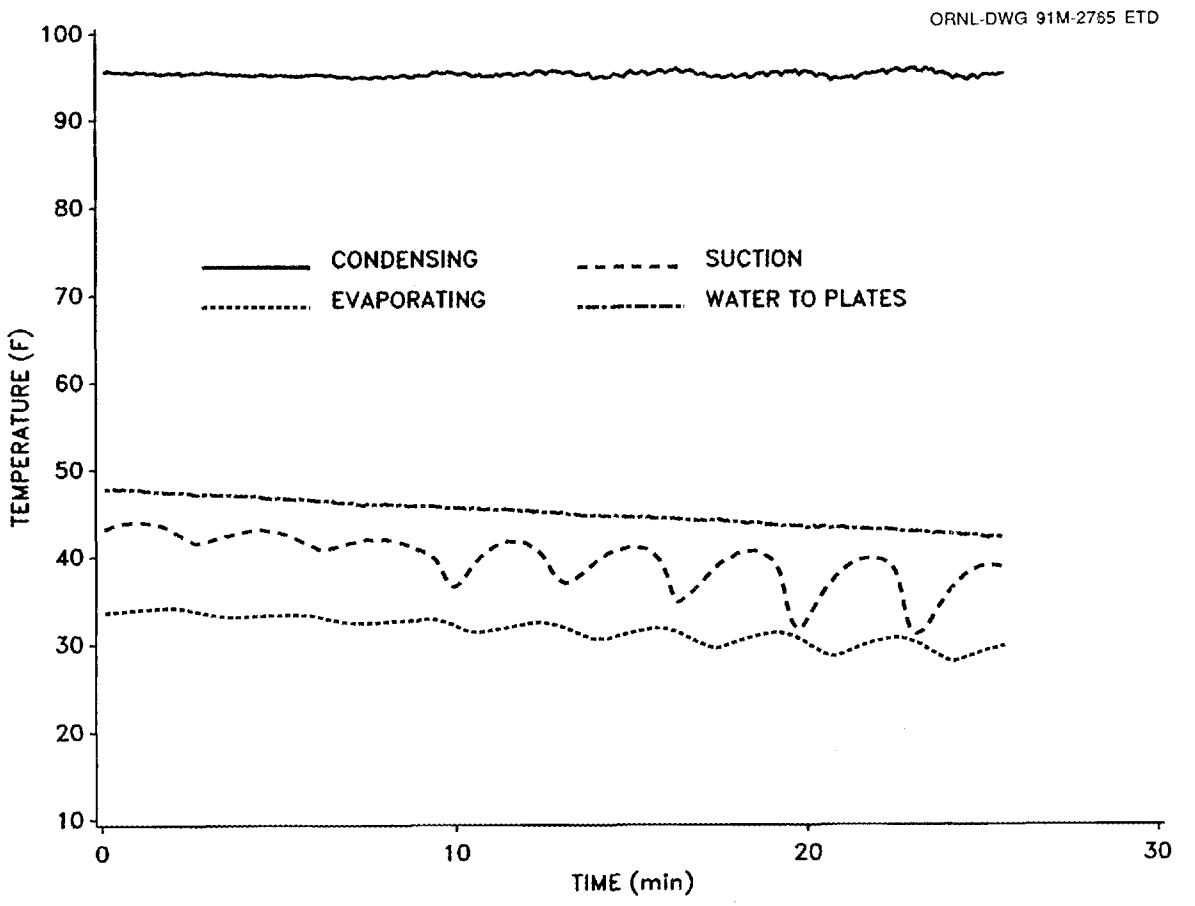

Fig. 6. Condensing, evaporating, suction, and water temperature during cooldown cycle under manufacturer's recommended operating conditions (test 1001.003). All temperatures are $\pm 0.5°F$.

temperature during the cooldown and ice-making modes is shown in Fig. 8. Figure 8 shows how the evaporating temperature decreases as ice builds up on the plate. It actually reaches its lowest value during the defrost period. This temperature drop is caused by mechanisms used for the defrost cycle; these include stopping the flow of liquid refrigerant from the condenser to the evaporator and forcing refrigerant from one set of plates into another.

The capacity of the system was calculated for each 6-s period during these tests (Fig. 9). The defrost cycle is clearly shown in this figure. The normalized capacity during the ice-making test is shown in Fig. 10. This latter figure more clearly shows the range of conditions under which the compressor operates, varying from -20 to 150% of the average capacity during ice making.

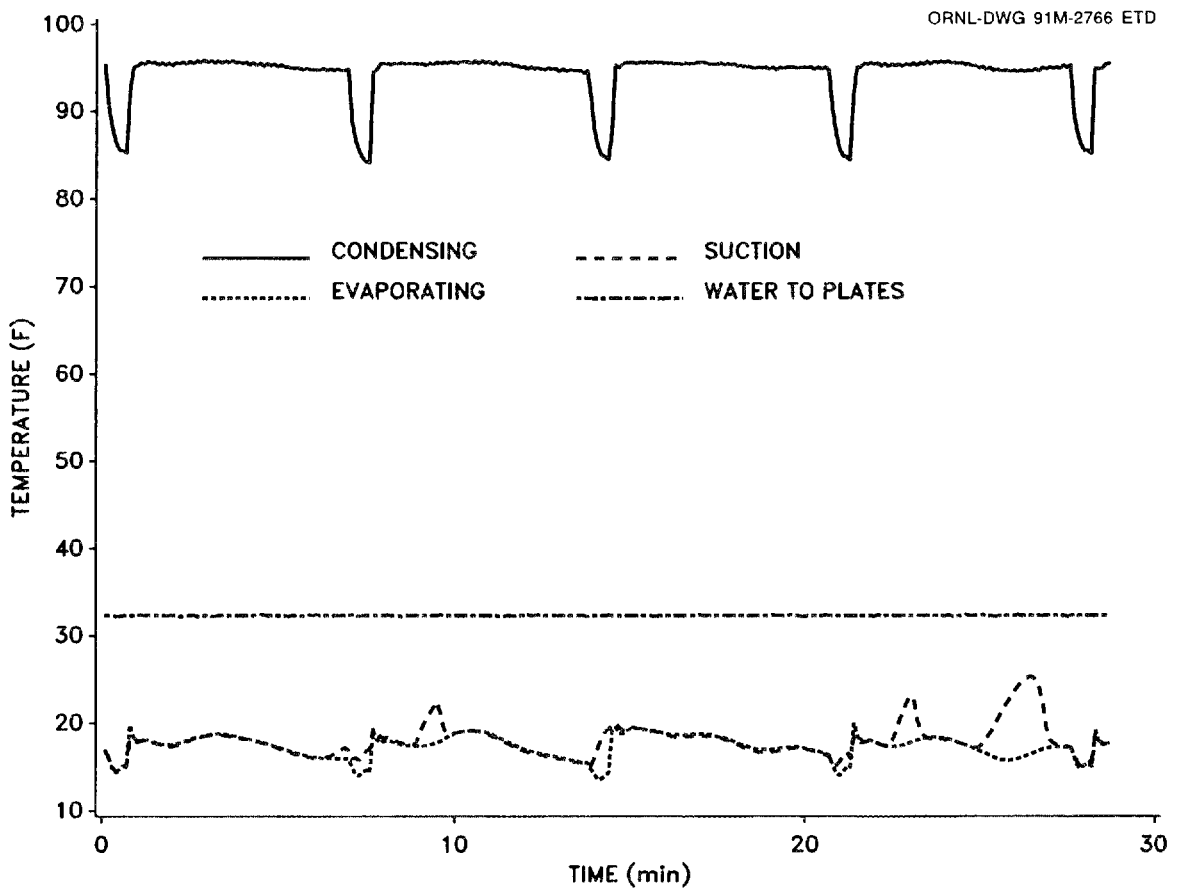

Fig. 7. Condensing, evaporating, suction, and water temperatures during ice-making cycle under manufacturer's recommended operating conditions (test 1002.002). All temperatures are $\pm 0.5°F$.

A large number of tests (listed in Table 5) were run to characterize the unit's performance as a function of compressor discharge pressure, compressor speed, defrost fraction, and distribution of defrost cycles. (The defrost fraction is equal to the defrost time divided by the sum of the defrost time and the ice-making time.) The distribution of the defrost cycles was varied as well as the defrost fraction because the distribution of the defrost cycles has a direct bearing on the maximum thickness of the ice layer. Those tests run at a compressor speed of 1550 rpm and with the original thermal expansion valves are summarized in Fig. 11. As expected, the capacity decreases with increasing defrost periods and with increasing condensing temperatures. It was hoped that these tests would reveal an optimum defrost schedule, one that would best balance the advantages of the dynamic cycle (i.e., the limit placed on the ice buildup and the resulting heat transfer resistance) and the

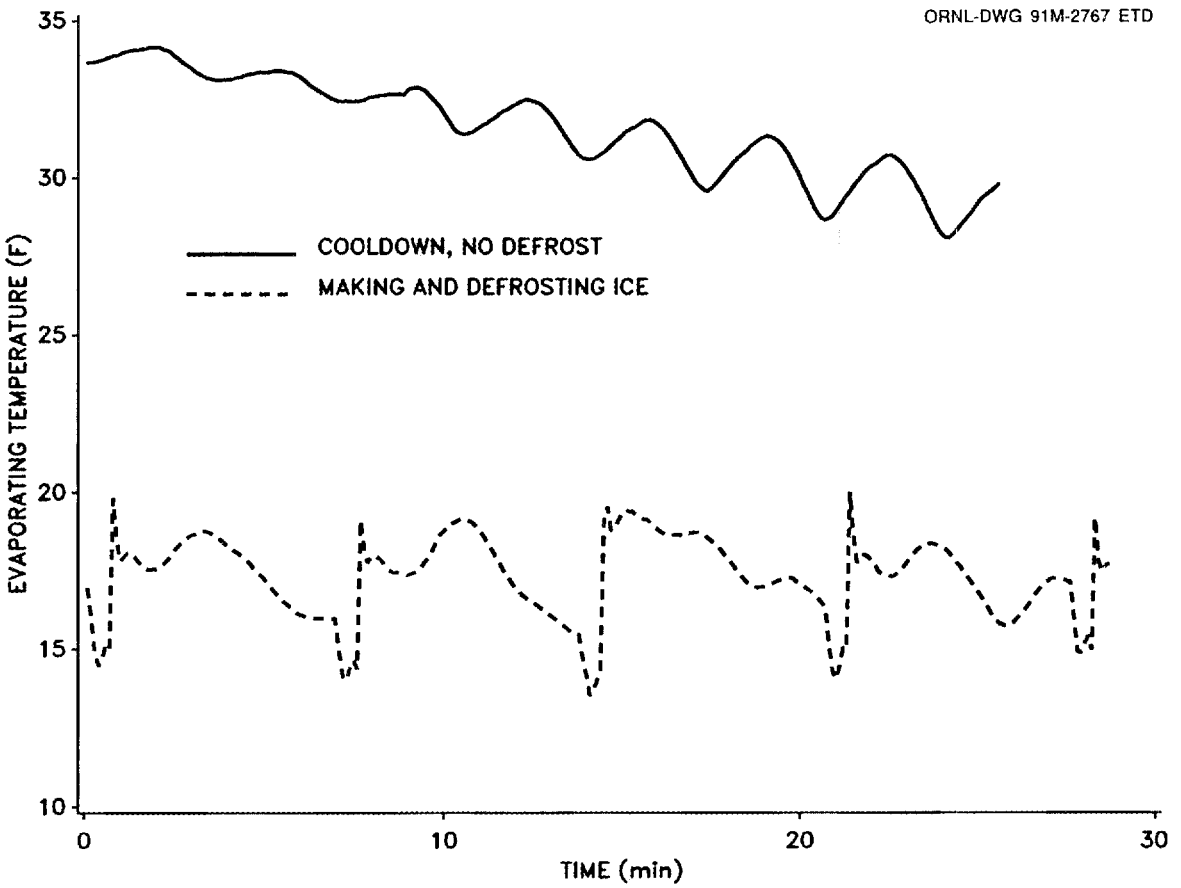

Fig. 8. Evaporating temperature during cooldown and ice-making cycles.

disadvantages (i.e., the introduction of the hot gas into the evaporator plates and the interruption of the flow of cold refrigerant to the plates). However, the tests here show a linear relationship between capacity and the defrost fraction. This is supported by the regression analysis discussed later. For this machine, the minimum defrost time is not determined based on a thermodynamic optimum, but rather on the minimum defrost necessary to clear the plates of ice. Testing showed that whenever the defrost fraction fell below 7%, the plates were not cleared of ice. This shows that the thermodynamic optimum is also a strong function of the physical design of the system, specifically of the spacing between the plates. The recommended defrost fraction is also shown on Fig. 11 to be 8.5%.

Multivariate regression analysis was used to analyze the results of over 100 separate tests. Several regression models were tested reflecting various combinations of the variables

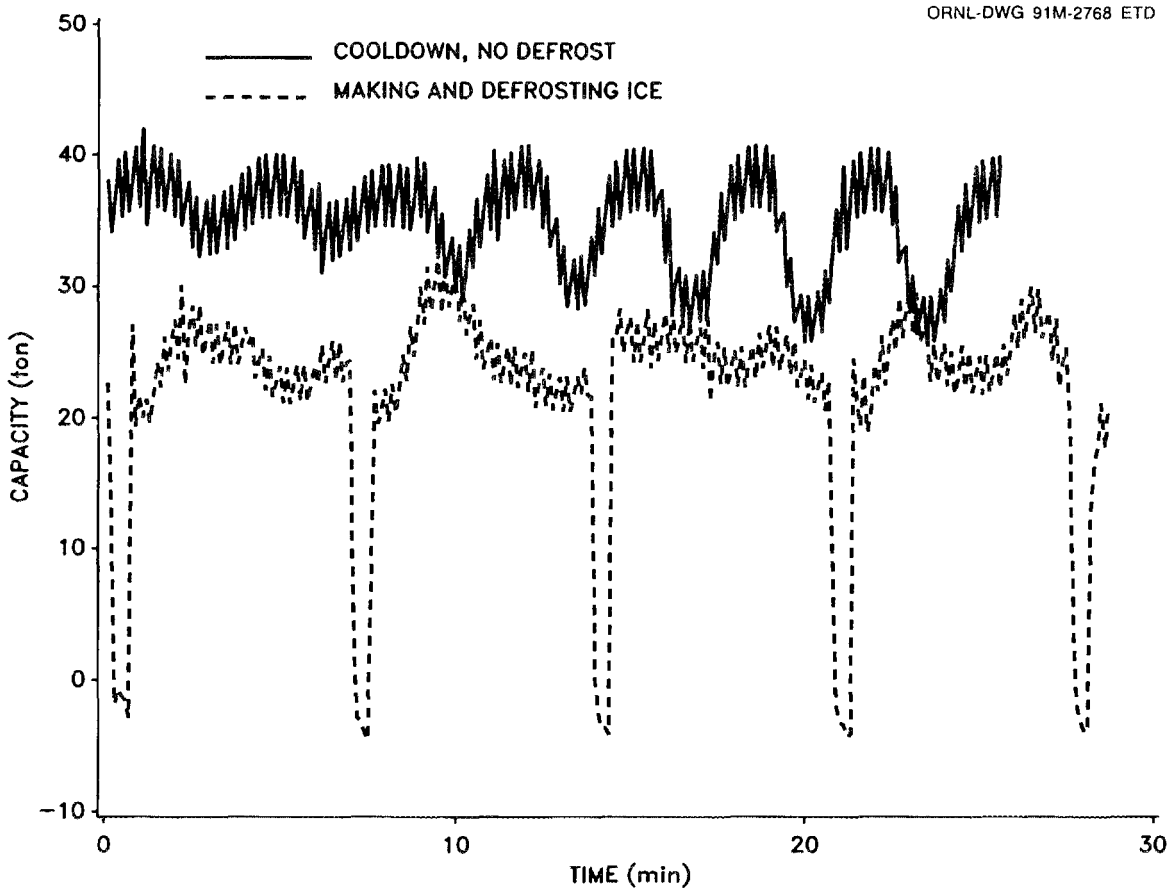

Fig. 9. Capacity of Turbo system under manufacturer's recommended operating conditions (tests 1001.003 and 1002.002).

listed in Table 7. The change in compressor speed was looked at both as a proportional variable (RPM) and as a step variable (Speed) but never both in the same model. The defrost fraction was modeled in combination with either the ice-making time or the defrost time, but all three were never included in the same model to avoid the use of collinear variables. The ice-making time and the defrost time were also modeled together without the defrost fraction variable. A variable, Inew, indicated which set of expansion valves were in use during the test.

Two models, one using the defrost fraction and the other using both defrost and ice-making times, were equally successful. Both of these models explained ~85% of the variations in the measured cooling rates, based on the adjusted multivariate coefficient squared (adj. R^2). In both models, all variable coefficients were statistically significant as

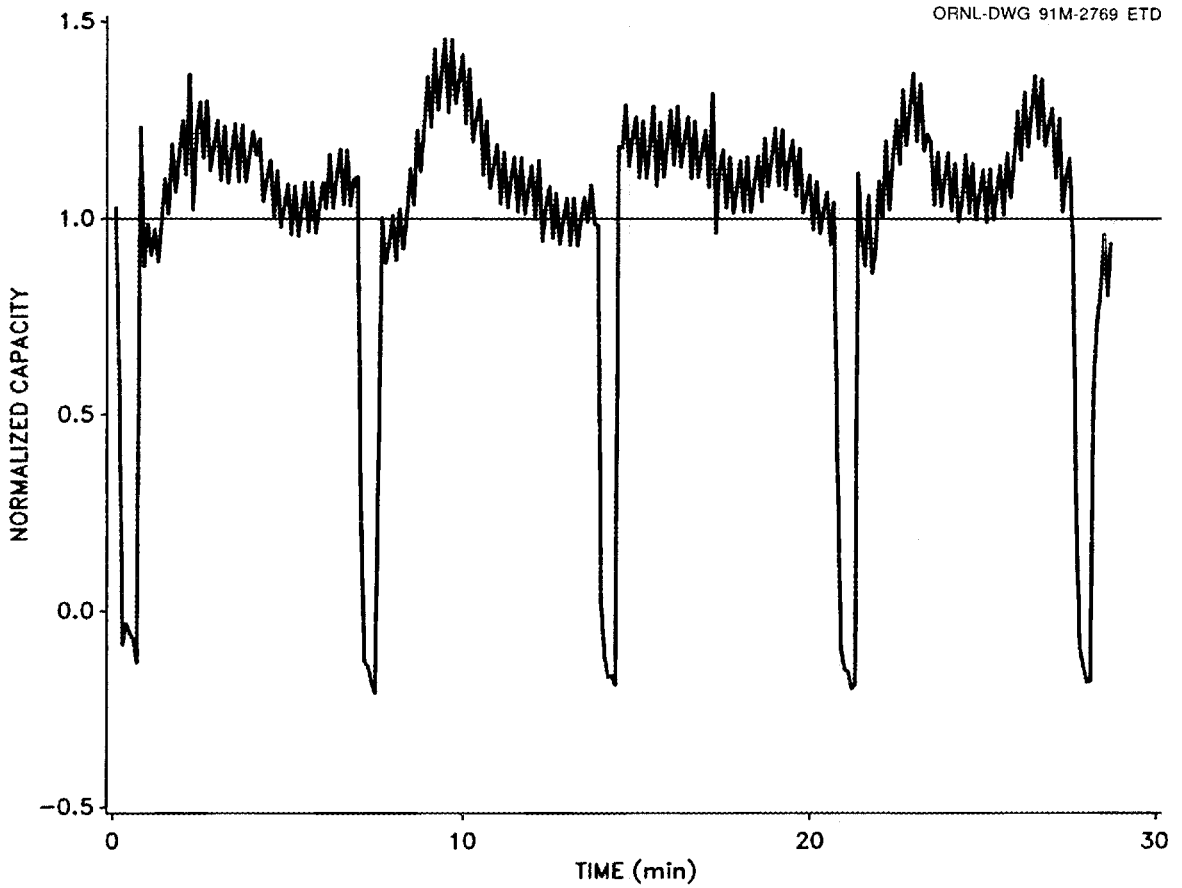

Fig. 10. Normalized capacity of Turbo system while making ice under manufacturer's recommended operating conditions (test 1002.002).

judged by the Student's T-test at the 97% confidence level. These models are shown in Eqs. (12) and (13), and the standard errors for each variable coefficient are shown in Table 8. Based on the similarity of these two models, it appears that the defrost fraction is an adequate performance predictor, so long as the defrost cycles are not spaced so far apart to initiate ice bridging between evaporator plates.

$$Re^* = 25.5 - 0.046 \times P_D - 0.059 \times t_D + 0.0049 \times t_I + 0.0033 \times RPM + 0.47 \times Inew , \quad (12)$$

$$Re^* = 27.2 - 0.045 \times P_D - 0.15 \times \tau_D + 0.0028 \times RPM + 0.47 \times Inew , \quad (13)$$

where

Re^* = refrigerating capacity (tons),

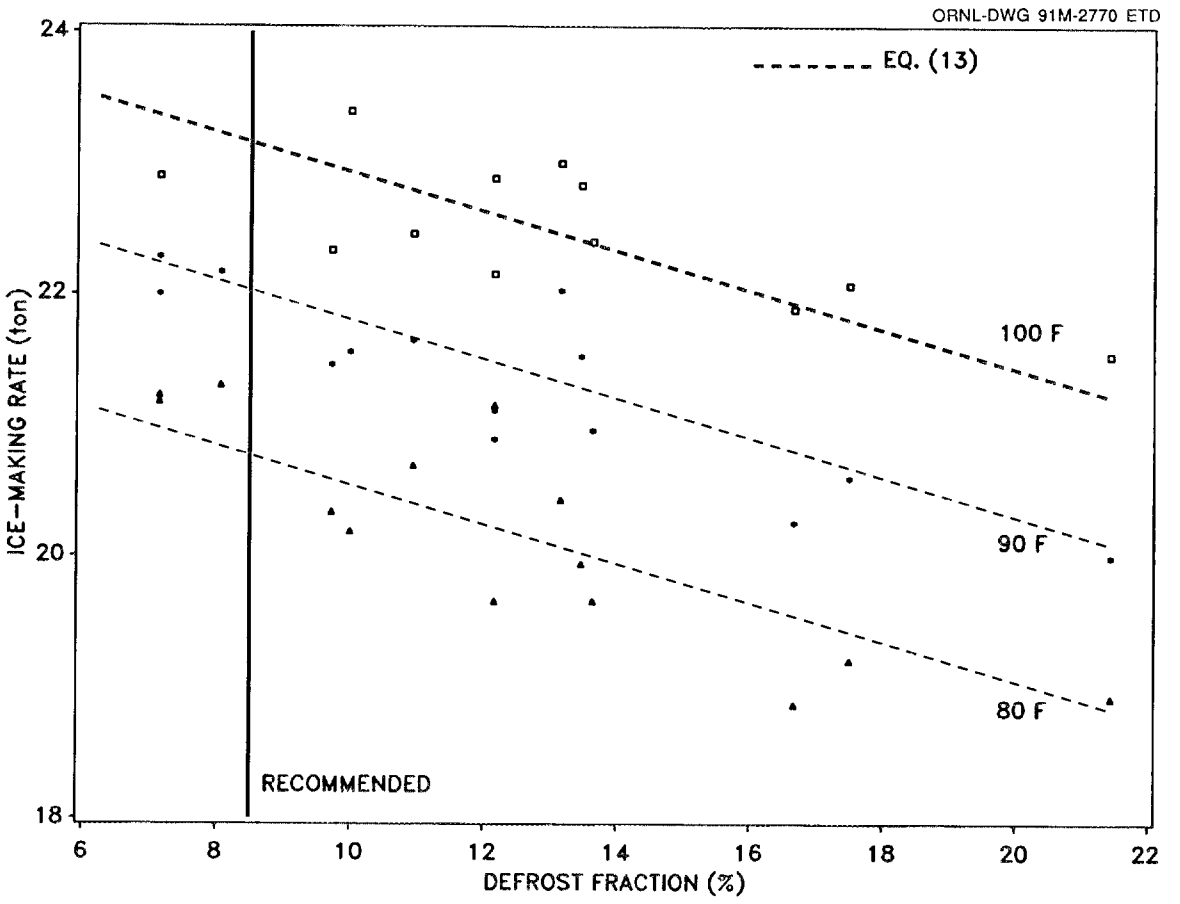

Fig. 11. System capacity measured during ice-making tests for varying condensing temperatures and defrost schedules with compressor speed of 1550 rpm and original thermal expansion valves.

P_D = compressor discharge pressure (psia),

t_D = time in defrost cycle for each plate (s),

t_I = time in ice-making cycle for each plate (s),

τ_D = defrost fraction $[\tau_D = 100 \times t_D/(t_D + t_I)]$ (%),

RPM = compressor speed (rpm),

Inew = 0 for original expansion valves, 1 for new valves.

These equations can be interpreted to mean that the ice-making rate of the unit is decreased ~0.045 tons for each increase in the discharge pressure of 1.0 psi. Figure 12 shows the relationship between capacity, condensing temperature (or compressor discharge pressure), and defrost schedule (the recommended schedule is 376-s ice making and 35-s

Table 7. Variable definitions for multivariate regression analysis of ice-making performance

Variable	Definition
Re^*	Cooling rate based on 6-s refrigerant measurements, ton
P_D	Discharge pressure at compressor, psia
t_D	Time in defrost cycle for each plate, s
t_I	Time in ice-making cycle for each plate, s
τ_D	Defrost fraction % [$= 100 \times t_D/(t_D + t_I)$]
RPM	Compressor speed, rpm
Speed	= 0 for compressor speed of 1550 rpm, = 1 for 1775 rpm
Inew	= 0 for original expansion valves, = 1 for new valves

Table 8. Variable coefficients and standard errors for multivariate regression analysis of ice-making performance

Variable	Coefficient	Standard error
	Eq. (12)	
Intercept	25.5	1.15
P_D	−0.046	0.0030
t_D	−0.059	0.0078
t_I	0.0049	0.0010
RPM	0.0033	0.00066
Inew	0.47	0.17
	Eq. (13)	
Intercept	27.2	1.21
P_D	−0.045	0.0030
τ_D	−0.15	0.017
RPM	0.0028	0.00064
Inew	0.47	0.17

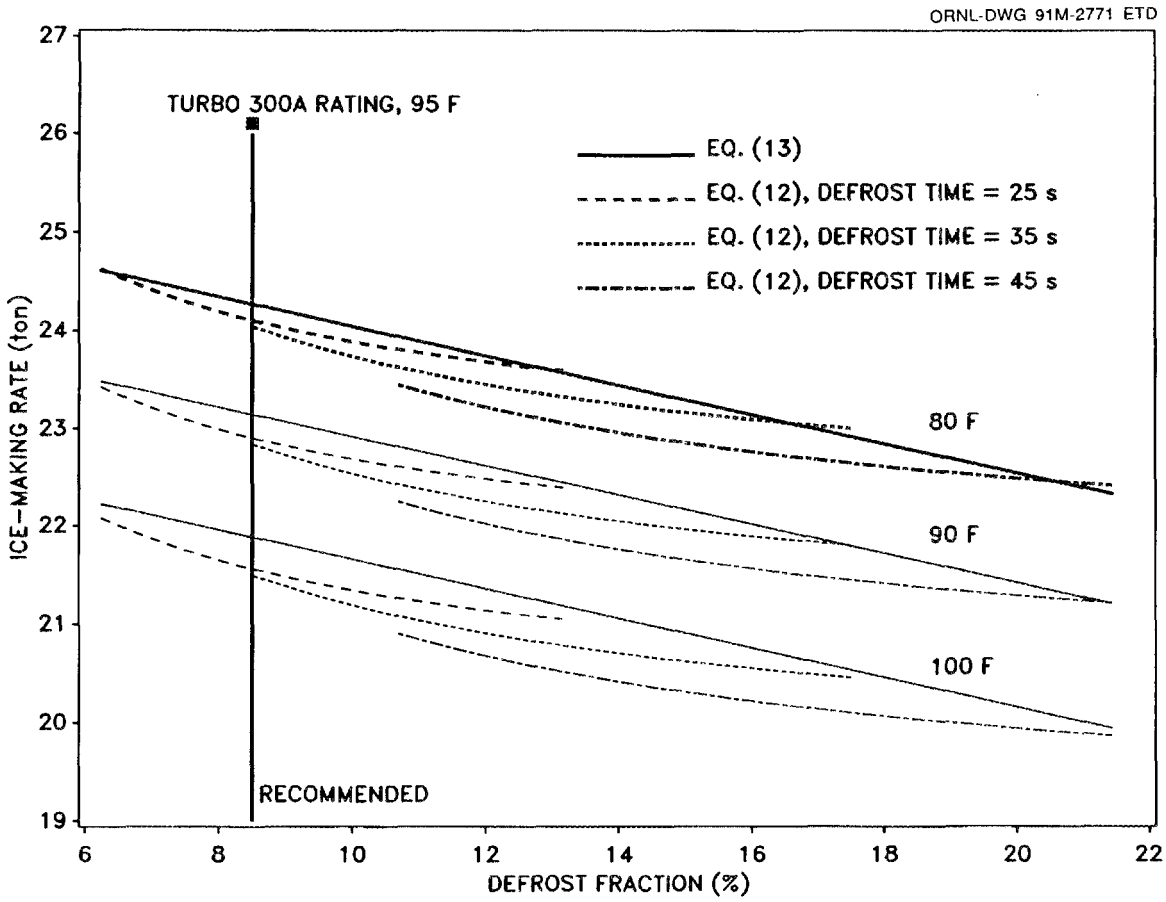

Fig. 12. Relationship between system capacity, condensing temperature, and defrost schedules for compressor speed of 1780 rpm with properly adjusted expansion valves.

defrost) for these two equations. This figure shows a linear relationship between the ice-making rate and percent of time in defrost as expected for Eq. (13). The relationship between percent of time in defrost and the ice-making rate for Eq. (12) is shown as a range based on defrost periods ranging from 25 to 45 s and ice-making periods ranging from 165 to 376 s. This range of values varies in width from 0 to 0.6 ton and the higher values agree quite closely with the values calculated using Eq. (13). Each increase of 1 rpm in the compressor shaft speed increases the ice-making rate by ~0.003 ton, or an increase of ~0.7 ton as the speed was increased from 1550 to 1775 rpm. The replacement expansion valves increased the capacity of the machine by almost half a ton. This serves to emphasize the importance of ensuring the proper adjustment and operation of these expansion valves throughout the operating life of any unit.

During the ice-catching test (described in Sect. 3.1), a condensing temperature of 90°F was maintained. The ice-catching test conditions combined a 35-s defrost cycle and a 225-s ice-making cycle. This combination places the unit in the defrost mode ~12% of the cycle time (the recommended defrost time is ~8.5% of the cycle time). This test was useful for comparing the ice production from each section (note that the ice production rate would be greater under the recommended operating schedule).

Ice released from the four ice-making sections of the Turbo machine was caught and weighed. The results of this test are presented in Fig. 13. The ice production of the four sections is relatively uniform. It slowly increases for all sections from the first cycle through the third as the overall tank temperature and therefore the temperature of the water supplied to the top of the plates is reduced.

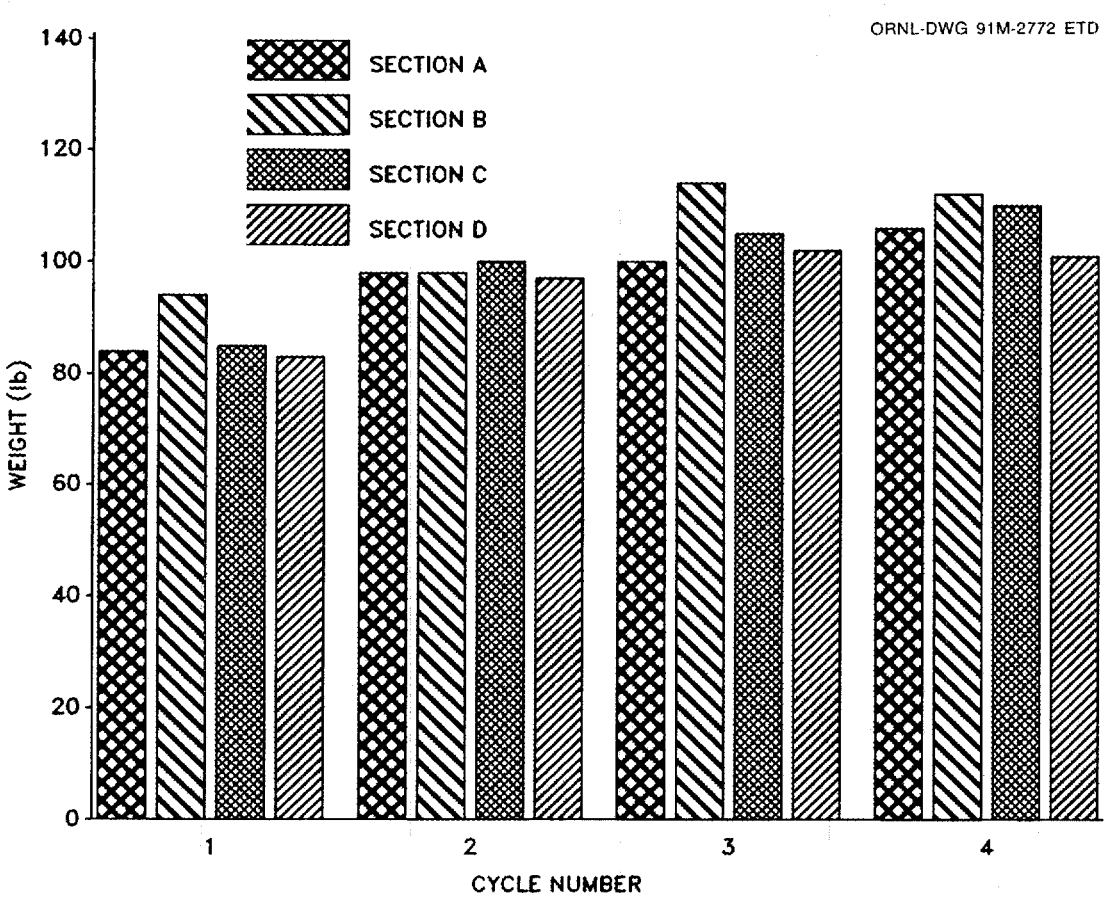

Fig. 13. Ice production in four evaporator sections during test at 35-s defrost cycle time and 225-s ice-making cycle time at condensing temperature of 90°F.

Auxiliary power is required for the circulation pump. The average pump power was ~2.7 kW. If a 30-ton system was running with compressor power consumption of 1.2 kW/ton, this additional power use would increase the overall power consumption to ~1.3 kW/ton, an increase of ~8%.

The Turbo unit tested was a model HP300-ASC. According to Turbo literature, model HP300-A is rated at 26.1 tons at 32°F water and 39.9 tons at 44°F water, both at 95°F saturated condensing temperature. Tests 1002.002 and 1001.003 were made at the manufacturer's recommended ice-making/defrost schedule with a saturated condensing temperature of 95°F and water inlet temperatures at the rated values of 32 and 44°F (see Figs. 6 and 7), respectively, and are therefore appropriate for comparison to these rated values. During the ice-making period, the Turbo unit operated at an average rate of 22.5 tons, or 86% of the rated value. During the cooldown period, the Turbo unit operated at an average rate of 35.2 tons while the water temperature to the plates varied from ~42 to 48°F, or 88% of the rated value. Part of this discrepancy can be explained by the previously discussed refrigerant flowmeter losses of 0.1 ton while making ice and 0.5 ton during defrost. (Note that these losses are not additive; that is, there will be a loss of 0.1 ton 91.5% of the time while liquid refrigerant is flowing to the evaporator and a loss of 0.5 ton 8.5% of the time while hot gaseous refrigerant is flowing to the evaporator.) An additional 0.4 ton is lost through the shell of the storage system as is discussed later in this report. The Turbo ratings are also based on compressor manufacturer ratings that can be 5% higher than actual compressor steady-state performance according to Air-Conditioning and Refrigeration Institute (ARI) rating standards. Figure 9 shows the capacity during both of these tests.

The Turbo tank was designed to store 212 ton-h of ice. The amount of ice stored in the tank [test 0803 from Eq. (1)] was 219 ton-h when the auto shut-off control stopped the compressor. Allowing for some standby losses during the charging period, the tank stored at or above its rated capacity.

The biological ice nucleator, Snomax™, was tested at two condensing temperatures, 90 and 100°F. It had no apparent effect on the operation of the dynamic ice maker. During the 90°F tests the power consumption was 1.16 kW/ton with the nucleator and 1.15 kW/ton without. During the 100°F tests the power consumption was 1.27 kW/ton with the nucleator and 1.28 kW/ton without. The evaporating temperature profiles were also examined and showed no clear difference between the cases with and without the nucleator. It is suspected that the period of time during which the nucleator could be expected to improve

performance, namely, when the water is at or below 32°F but ice has not started to form, is relatively short. Also, the shape or roughness of the plates might provide adequate nucleation sites in the absence of the nucleating agent.

5.2 DISCHARGE PERFORMANCE

The discharge (ice-melting) tests were listed in Table 6. Both of these tests were run until the ice was completely melted. Comparison of Tables 3 and 6 shows many tests that were not performed on the Turbo unit. Only one water flow rate, 90 gpm, and one discharge rate, ~95 kW, were tested. Therefore, this report cannot cover the total likely range of discharge conditions. However, the two tests reported here showed consistent performance and clearly define the available energy under one common set of operating parameters.

As described in Sect. 4.3, the discharge capacity was measured in three different ways. Figure 14 shows the relative consistency of these different values in revealing the discharge

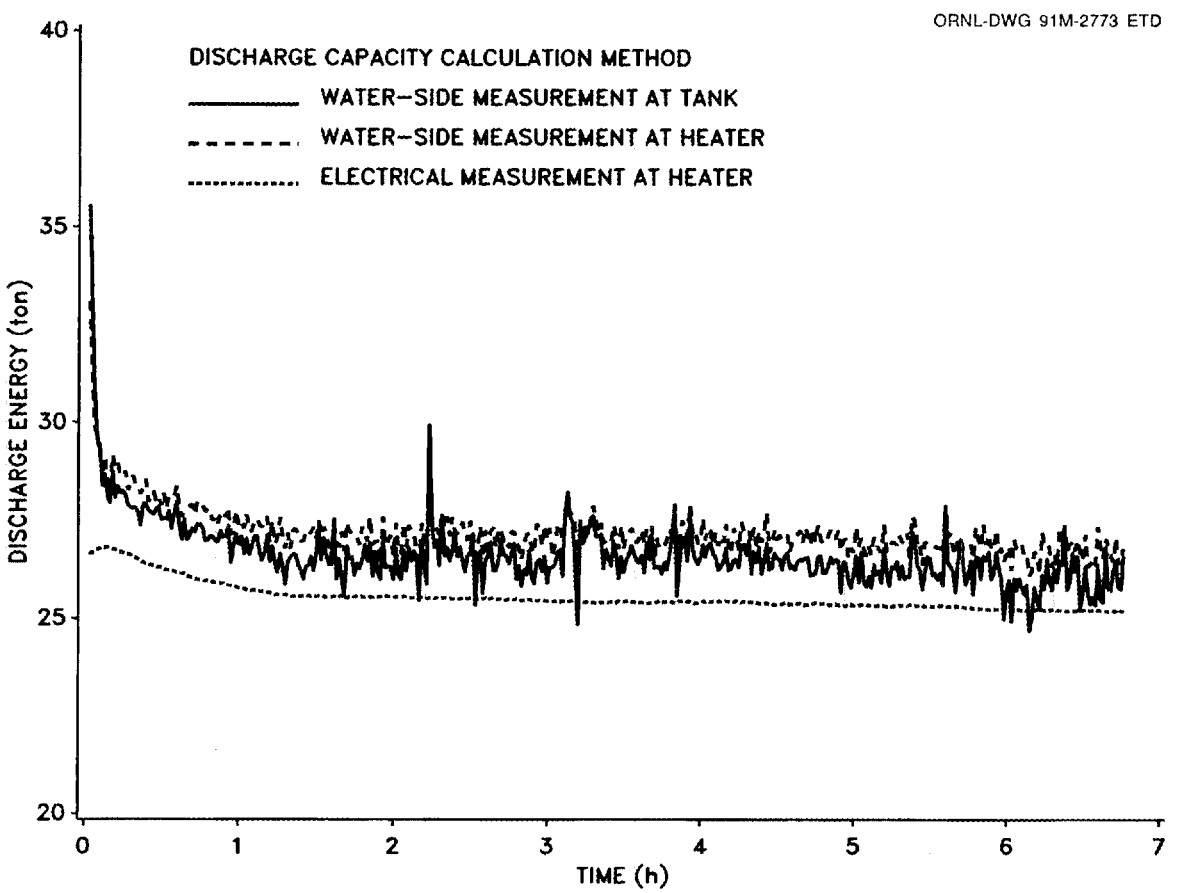

Fig. 14. Comparison of three different methods of measuring discharge capacity.

capacity available from the ice tank. The heater energy measurements are low due to inaccuracies caused by the electrical controller used to select the heater power level. The water-side measurement at the heater should be slightly less than the water-side measurement at the tank due to heat gains by the circulation pumps. Figure 15 shows that the cumulative discharge energy removed from the ice tank during these two tests reached ~200 ton-h.

The discharge performance tests generally showed that the ice stored within the Turbo tank was completely available for discharge at temperatures <45°F. At the end of the discharge tests, there was never more than ~1/2 ft^3 of ice floating within the tank. The only other unavailabilities result from heat gains to the tank and piping, discussed in the next section, and the friction losses in the piping, overcome by the circulating water pumps. The circulating pumps were used, in addition to the pumps located near the heater (see Fig. 2), to increase the flow to the water distribution headers in the storage tank. This additional

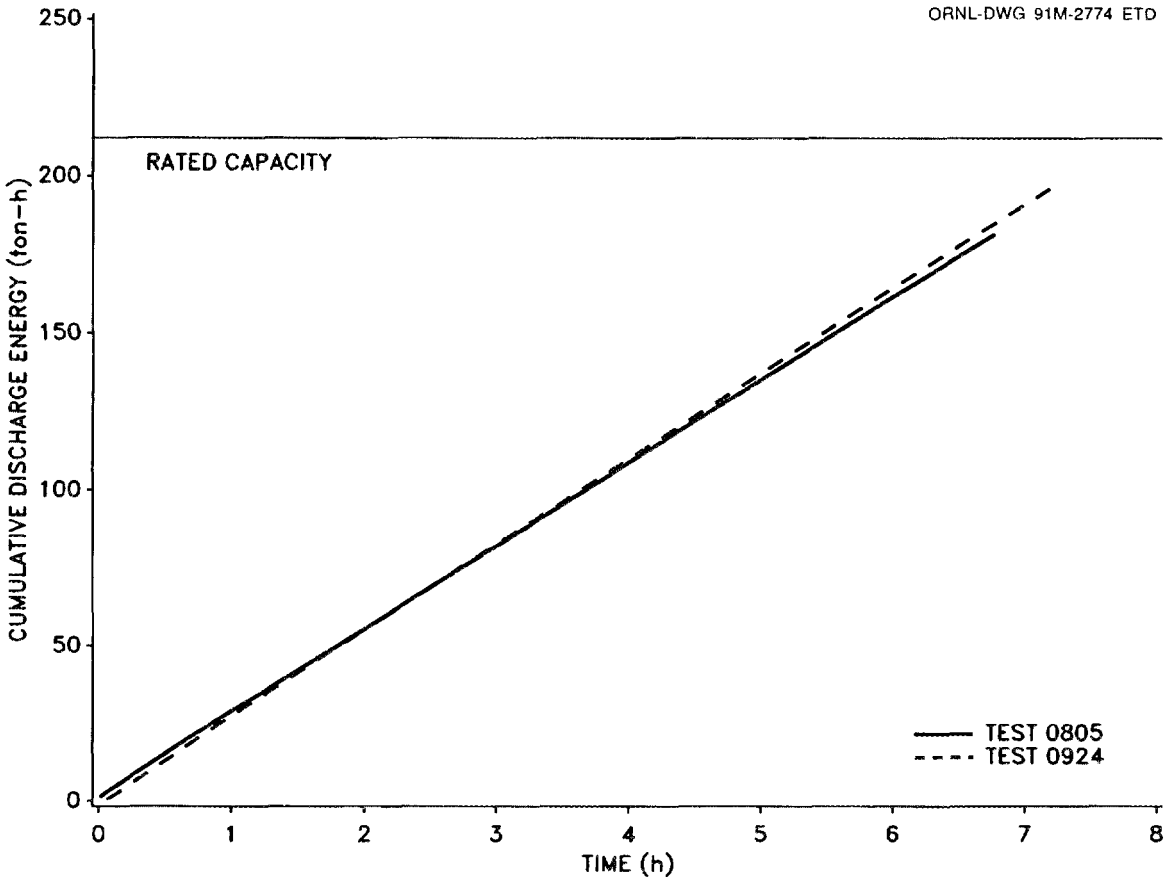

Fig. 15. Cumulative discharge energy during discharge tests 0805 and 0924.

flow was necessary to adequately agitate the tank. The total circulating pump power amounted to 11.3 ton-h over a 7.5-h discharge test.

Each discharge test lasted ~7 h. The top surface of the tank was visually inspected throughout the test period. The ice melted first in the center of the tank because that was where the water dropped down from the circulation header. Eventually, however, the ice near the edges was undercut and fell into the water in the tank. The water leaving the bottom of the tank was below 40°F during most of the test as can be seen in Fig. 16 (tests 0805 and 0924). The temperature begins to rise near the end of the test as the ice is depleted and the load is met by the sensible cool storage in the water up to the maximum temperature of 45°F.

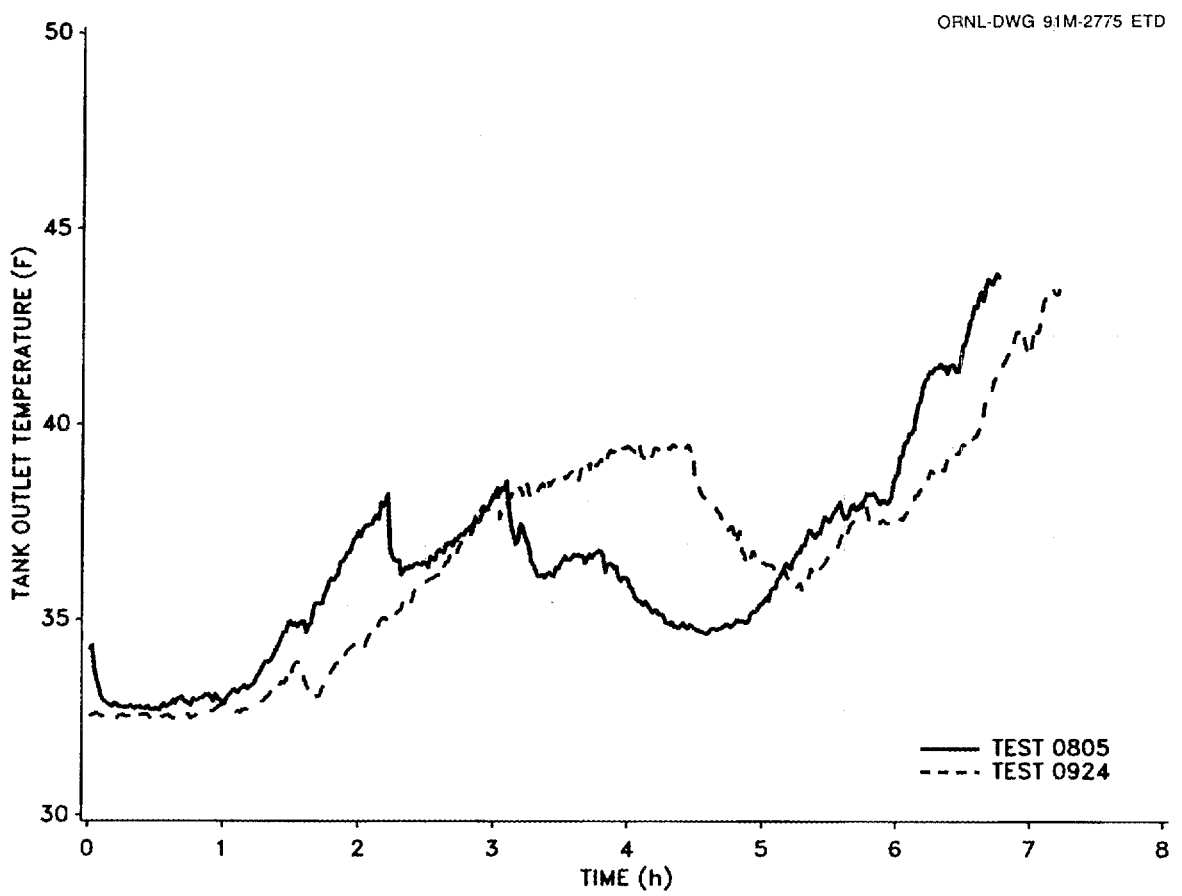

Fig. 16. Temperature of water leaving Turbo tank during two discharge tests. All temperatures are ±0.5°F.

5.3 STANDBY HEAT GAINS

Standby heat gains were measured in tests with the tank charged with ice and in tests with the tank charged with chilled water. The standby losses were measured in two ways as was described in Sect. 3.3. The method of continuously measuring the tank drainage was less successful because the amount of water trapped in the ice was large relative to the melting rate. However, although this method failed to give a direct measure of the melting rate for short periods of time, its results over the total test period agreed closely with the results of the test method based on measuring the rise in the tank water temperature. These losses were measured to be 0.3 to 0.4 ton for water above freezing temperatures during the first test and ~0.47 ton for a tank full of ice during the second test. These losses represent ~2% of the capacity of the unit during ice making. Based on the rated capacity of 212 ton-h, this loss rate can be expressed as 0.002 ton/ton-h, or alternatively, it would take 530 h (22 d) for a fully charged tank to melt.

It is interesting to estimate where (and how) the standby losses occur. Turbo specified a minimum tank wall and floor insulation of 3 in. of polyurethane foam.[10] The total heat conductance (UA) value for these areas is therefore 20.9 Btu/h-°F or 0.00174 ton/°F, a very small amount. For a temperature difference of 40°F, as in the second standby-loss test, this amounts to only 0.066 ton. The top loss is more difficult to estimate. Essentially, the top structure housing the evaporator plates acts as a fin by increasing the heat loss area; also, the insulation is not as thick in these walls. Even accounting for these factors and assuming that the top structure is insulated with 1 in. of urethane, the additional heat gain through the top structure would be only ~0.09 ton. The total estimated conductive heat gain is then only ~0.15 ton, out of a measured gain of ~0.4 ton.

The most likely explanation for this difference lies in a small amount of water vapor condensation. Even with the top doors closed, there is likely to be some air leakage. If the remaining 0.25 ton of heat gain is attributed to water condensation, it would amount to 2.8 lb/h or 0.33 gal/h. This small amount would not be noticed in a total tank volume of 5250 gal and a working inventory of 3400 gal of water.

5.4 POWER CONSUMPTION

The Turbo unit required a larger power consumption than was expected. The Turbo 300-A is nominally rated at 25.8 kW while making ice and 28.4 kW with 50°F water on the

plates. The predicted values are based on a cycle balance that correctly includes defrost losses and accurately predicts the amount of refrigeration produced by the unit. The power consumption prediction relies on compressor manufacturer's data for the average suction and discharge conditions. The compressor manufacturer's data is stated to be within 5% on the capacity and within 5% on the power use. Since the compressor manufacturer's power use data is stated in terms of bhp (rather than kW/ton or bhp/ton as is required with larger units), these accuracy margins can introduce errors that can be compounded to produce as much as a 10% error in the power consumption on a kW/ton basis. Also, as was seen in Fig. 7, the compressor is not operating under steady-state conditions while the unit is making ice. The variability of the suction and discharge conditions may make direct application of steady-state compressor test data inappropriate.

The motor efficiency further increases the power use above that required by the compressor. Any improvement in the motor efficiency (the installed motor had a nameplate rating of 88%) would directly translate to lower power consumption requirements. A belt-drive was used on the compressor-motor set so different compressor speeds could be tested. This coupling was checked by measuring the compressor and motor shaft speeds to detect any possible belt slippage. For equal-size sheaves on motor and compressor, the readings on a strobe tachometer matched exactly at 1780 rpm. Also, there was no heat generation near the belt (i.e., it was cool to the touch), which would also indicate a lack of slippage or energy dissipation. Therefore, it was assumed that there was no loss in shaft power from the electrical motor to the compressor.

During the Turbo cooldown test at the recommended defrost schedule and condensing temperature of 95°F, with carefully adjusted expansion valve settings (shown in Fig. 17), the unit required 1.05 kW for each ton of refrigeration, including the circulation pump. Without the water-circulation pump, the unit required 0.97 kW/ton of refrigeration (the HP300A is nominally rated at 0.64 kW/ton for this condition).[3] During a Turbo ice-making test at the recommended defrost schedule and condensing temperature of 95°F with carefully adjusted expansion valve settings (shown in Fig. 17), the unit required a total of 1.49 kW/ton. Without the circulating pump, the power consumption was 1.36 kW/ton (the HP300A is nominally rated at 1.0 kW/ton for this condition).[3] At a condensing temperature of 90°F at the recommended defrost schedule, the compressor requires 1.27 kW/ton, and the total power use was 1.4 kW/ton. For all these figures, the capacity was calculated from refrigerant pressure and temperature measurements described in Sect. 4.2 and shown in Eq. (1).

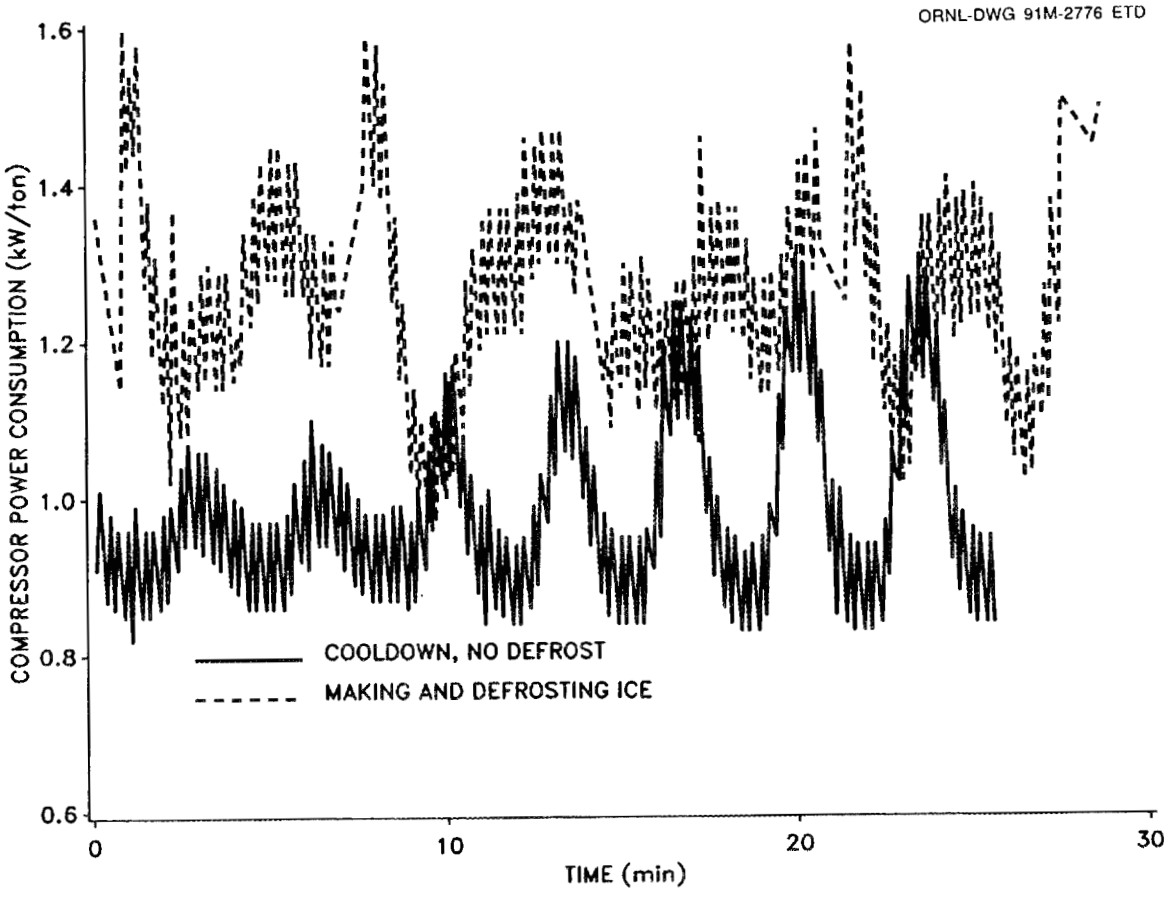

Fig. 17. Compressor power consumption during cooldown and while making ice at manufacturer's recommended operating conditions (tests 1001.003 and 1002.002).

The power consumption was analyzed using multivariate regression of over 100 separate tests, most of which are shown in Figs. 18 and 19 (where the recommended defrost fraction of 8.5% is also shown). All the independent variables listed in Table 7 were tested during this analysis. The results are shown in Eqs. (14)–(17). Table 9 shows the standard errors for the coefficients in these equations; all errors were statistically significant at the 98% confidence level. The adjusted multivariate correlation coefficient squared for all four equations was 0.95 or better; that is, at least 95% of the variation in the power consumption among the performance tests is explained by these equations.

$$PC_t = -0.95 + 0.0062 \times P_D + 0.0038 \times t_D - 0.00037 \times t_I + 0.00071 \times RPM - 0.033 \times Inew , \quad (14)$$

$$PC_t = -1.07 + 0.0062 \times P_D + 0.010 \times \tau_D + 0.00074 \times RPM - 0.034 \times Inew , \quad (15)$$

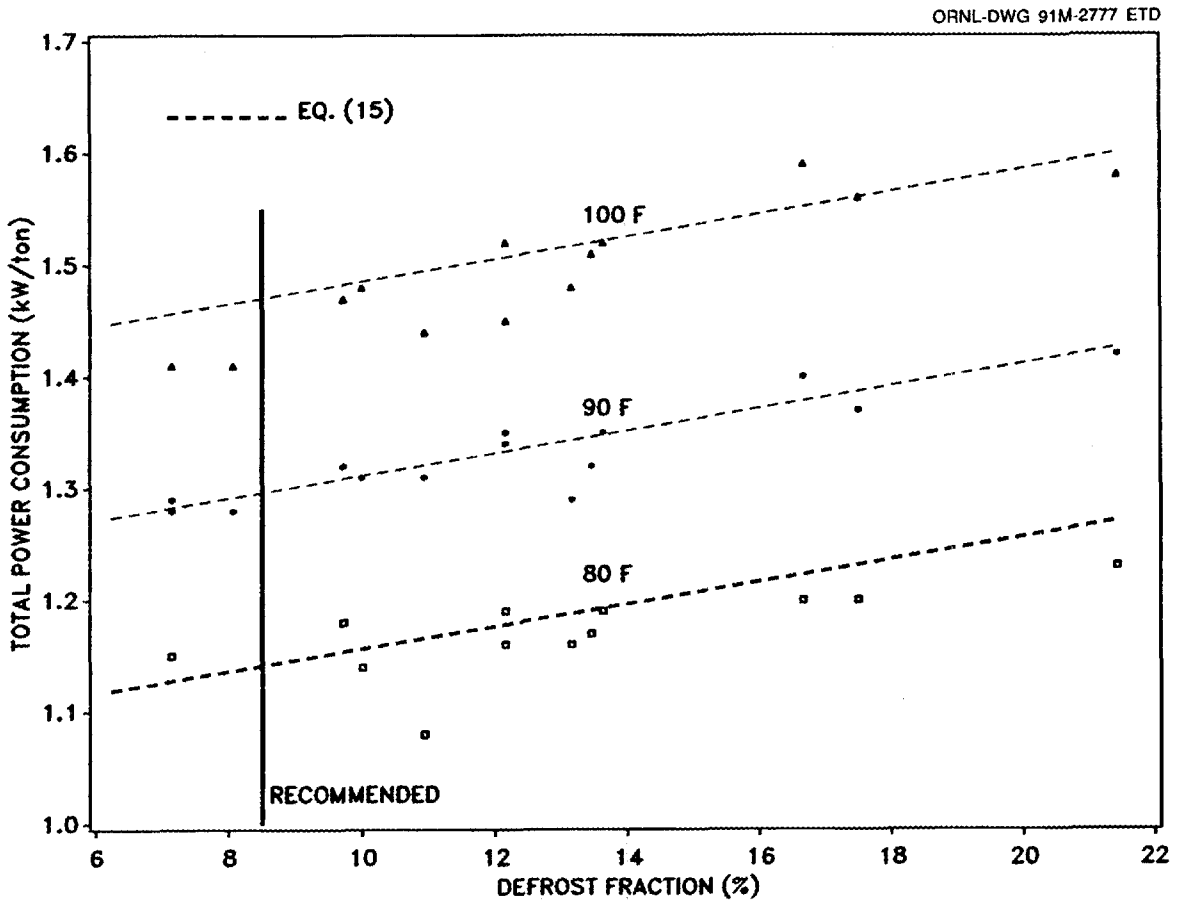

Fig. 18. Total power consumption during ice making for varying condensing temperatures and defrost schedules with compressor speed of 1550 rpm and original thermal expansion valves.

$$PC_c = -1.01 + 0.0058 \times P_D + 0.0034 \times t_D - 0.00033 \times t_I + 0.00072 \times RPM - 0.028 \times Inew, \quad (16)$$

$$PC_c = -1.12 + 0.0057 \times P_D + 0.009 \times \tau_D + 0.00074 \times RPM - 0.030 \times Inew, \quad (17)$$

where PC_t is the total power consumption including the circulating pump, kW/ton, and PC_c is the compressor power consumption, kW/ton.

Equations (14)-(17) show that the power consumption is increased by about 0.0007 kW/ton for each increase of 1 rpm in the compressor speed, or by 0.2 kW/ton as the speed was increased from 1550 to 1775 rpm. Increases in the discharge pressure also increase the power consumption, as was expected, and are shown in Figs. 20 and 21. The energy penalty associated with the defrost cycle is also shown in these equations by the positive

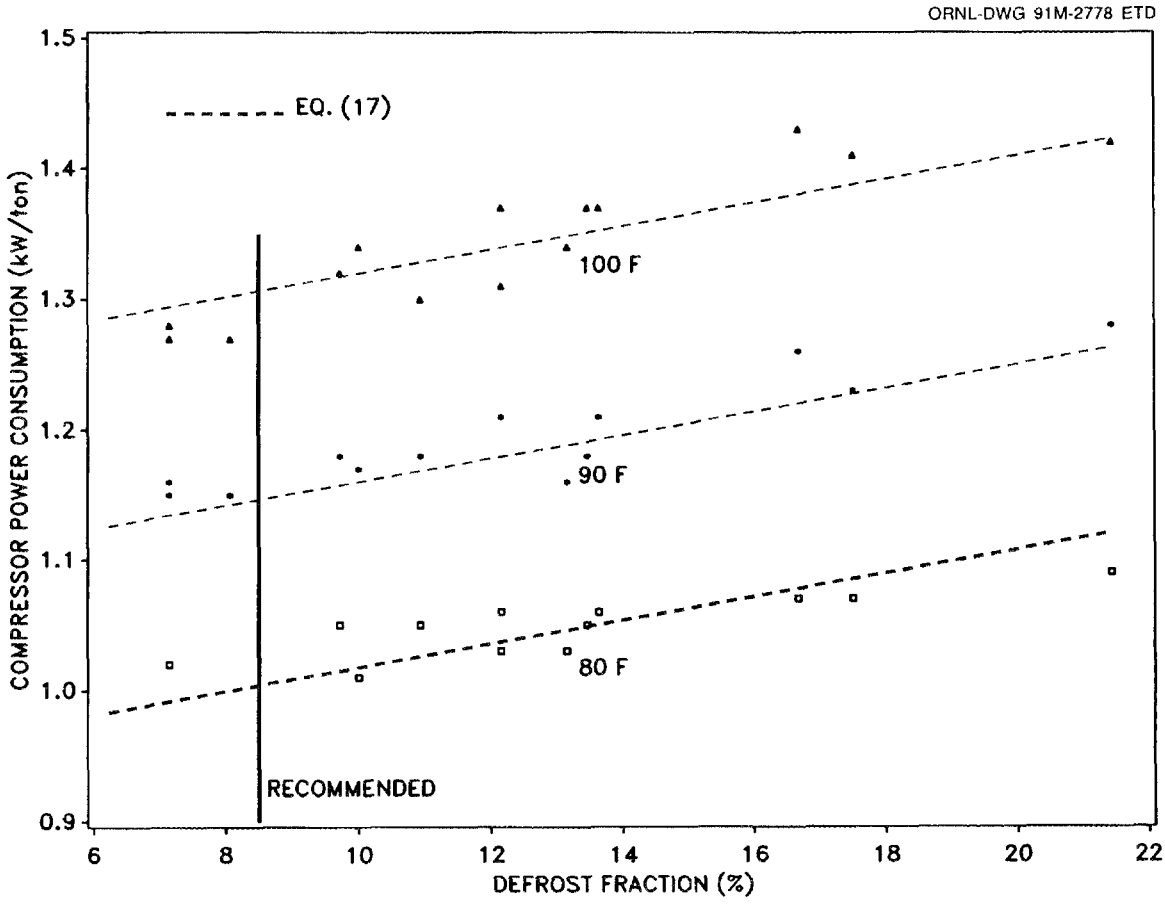

Fig. 19. Compressor power consumption during ice making for varying condensing temperatures and defrost schedules with compressor speed of 1550 rpm and original thermal expansion valves.

coefficients for t_D and τ_D. The recommended defrost schedule for this machine is 376-s ice making and 35-s defrost. Properly adjusted expansion valves can lower power use by ~0.03 kW/ton. The relationships shown in Eqs. (14)–(17) are for ice-making conditions only, that is, when the water at the top of the plates is ~32°F. At higher water temperatures, the unit is more efficient because the evaporating temperature is greater and because the unit does not go through the defrost cycle. Several tests were therefore made to determine the power necessary to chill the water at higher temperatures. Figure 22 shows the results of three cooldown tests. The test requiring the largest amount of power was made at a condensing temperature of 100°F, an ice-making time of 325 s (the recommended ice-making time is 376 s), and a defrost time of 35 s (equal to the recommended value). The compressor

Table 9. Variable coefficients and standard errors for multivariate regression analysis of power consumption during ice making

Variable	Coefficient	Standard error
	Eq. (14)	
Intercept	−0.95	0.084
P_D	0.0062	0.00022
t_D	0.0038	0.00057
t_I	−0.00037	0.000074
RPM	0.00071	0.000048
Inew	−0.033	0.013
	Eq. (15)	
Intercept	−1.07	0.067
P_D	0.0062	0.00022
τ_D	0.010	0.0012
RPM	0.00074	0.000045
Inew	−0.034	0.012
	Eq. (16)	
Intercept	−1.01	0.070
P_D	0.0058	0.00018
t_D	0.0034	0.00048
t_I	−0.00033	0.000062
RPM	0.00072	0.000040
Inew	−0.028	0.011
	Eq. (5)	
Intercept	−1.12	0.074
P_D	0.0057	0.00018
τ_D	0.0092	0.0010
RPM	0.00074	0.000038
Inew	−0.030	0.010

power use for this case is seen to vary from ~1.2 kW/ton for 50°F water to 1.5 kW/ton as the machine begins to make ice. Another test using this same defrost schedule (9.7% defrost) was made at a condensing temperature of 90°F as the water temperature dropped from 47°F, where the compressor power use was ~0.95 kW/ton, to the freezing point, where power rose to 1.4 kW/ton. This test shows a sharp increase in power use at a water temperature of

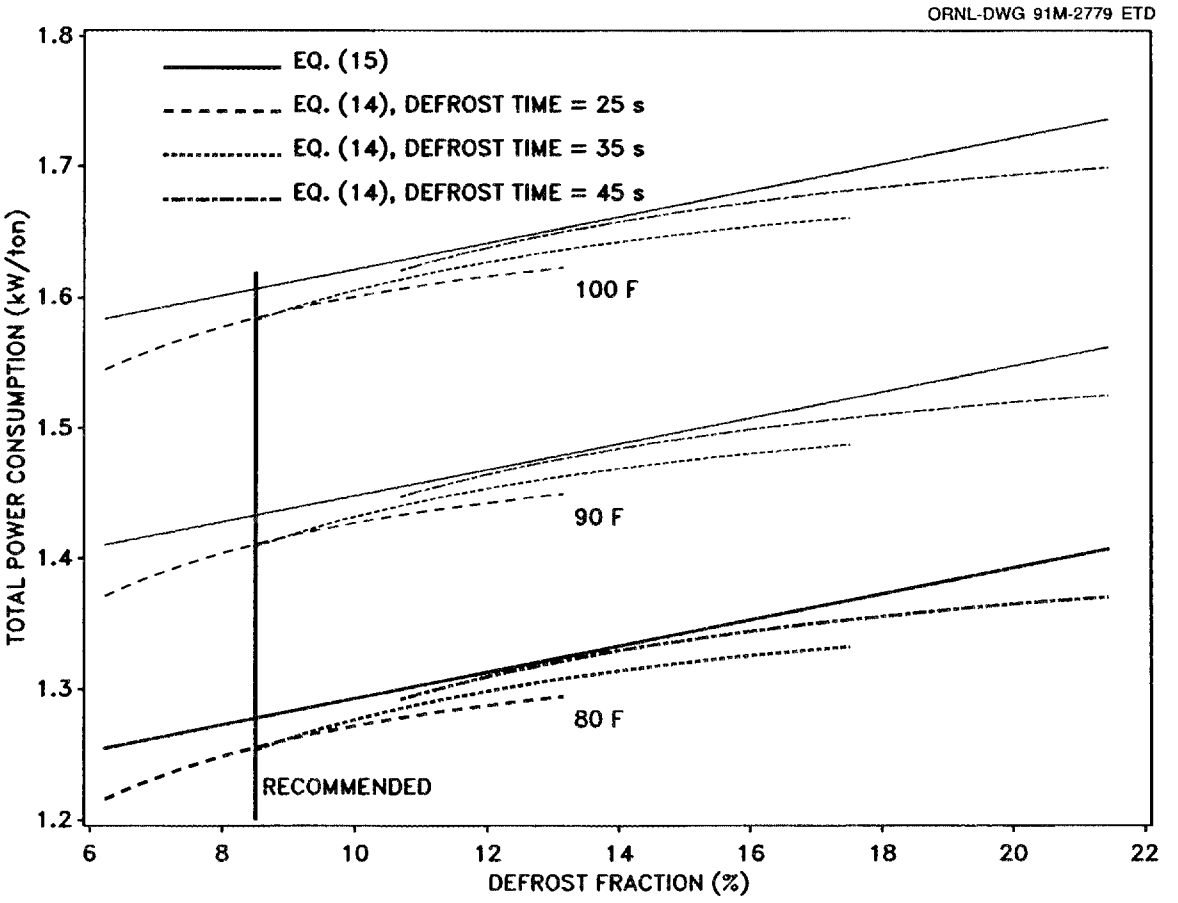

Fig. 20. Relationship between total power consumption, condensing temperature, and defrost schedules for 1780-rpm compressor speed with properly adjusted expansion valves.

~38°F, where the unit typically begins to go through the defrost cycle. At the manufacturer's recommended defrost schedule of 376-s ice making and 35-s defrost (8.5% defrost) at a condensing temperature of 95°F, the compressor required ~0.95 kW/ton with 47°F water to the plates, increasing to 1.36 kW/ton as the water temperature drops to 32°F, as was described previously.

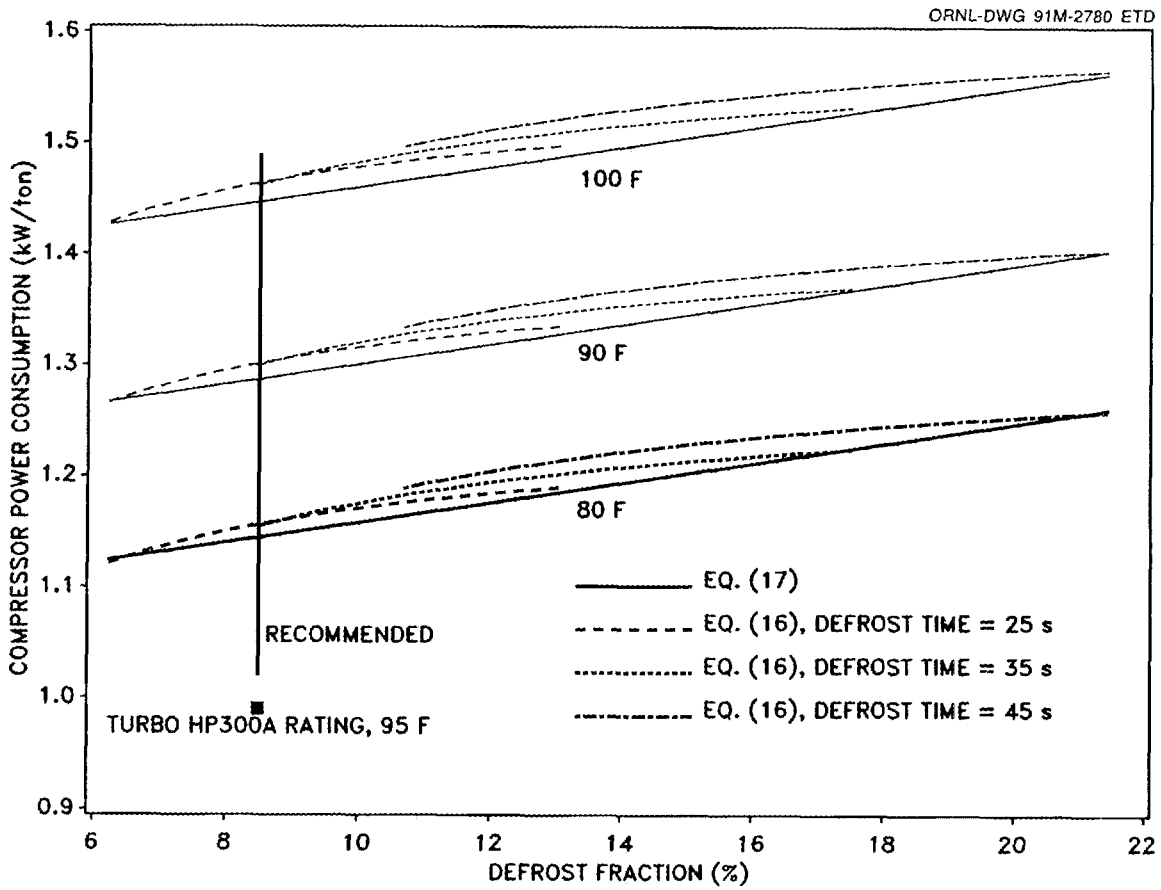

Fig. 21. Relationship between compressor power consumption, condensing temperature, and defrost schedules for 1780-rpm compressor speed with properly adjusted expansion valves.

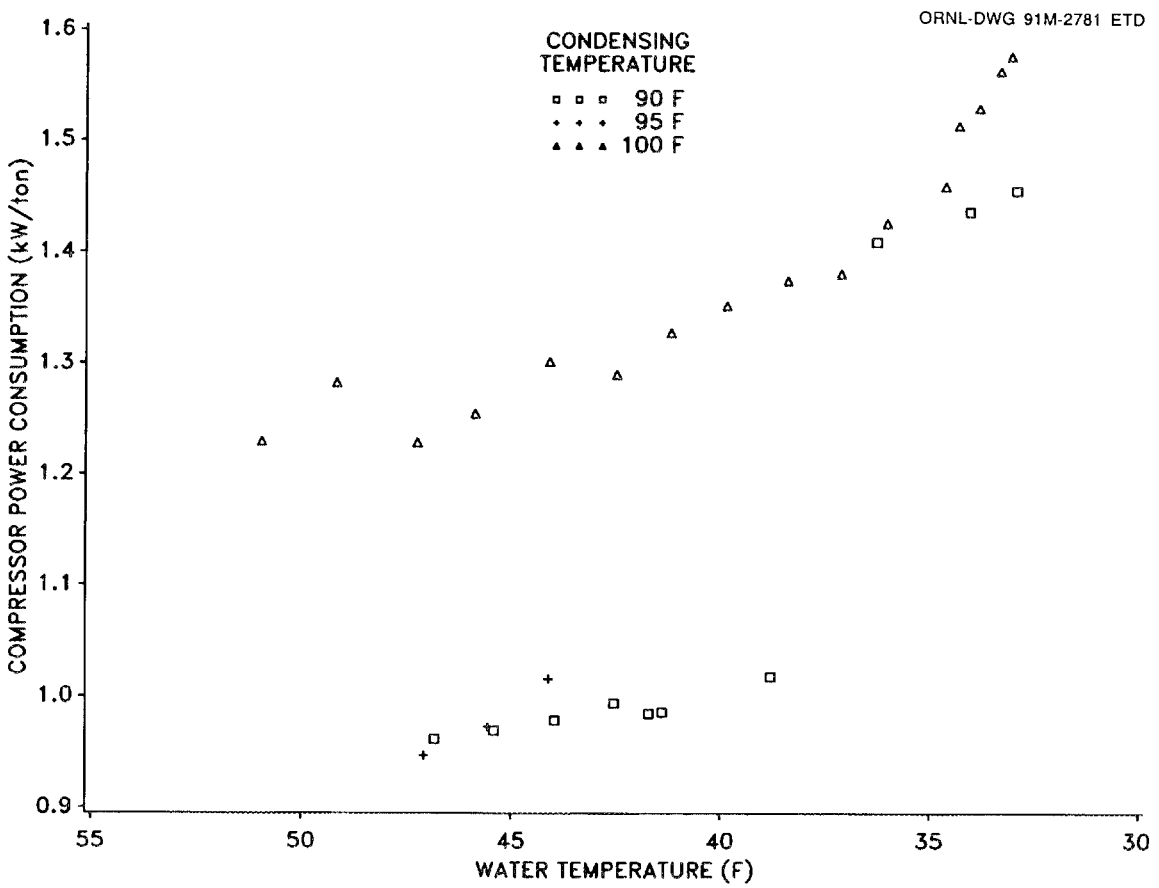

Fig. 22. Compressor power use while chilling water.

6. CONCLUSIONS AND RECOMMENDATIONS

Under recommended operating conditions, the Turbo unit showed the ice-making capability expected. The ice was uniformly produced and released from the evaporator sections and showed the expected mounded shape of ice within the storage tank. The unit's shut-off device worked properly when the unit was fully charged. A wide range of operating conditions were tested, and statistical analysis was used to represent the performance as a function of several key operating parameters. This characterization should prove useful in determining the expected performance of the system at conditions other than those rated in the literature.

Although the discharge tests were limited in scope they showed that the cool stored in the Turbo tank is completely available under a common discharge scenario. Visual observations made during these and other partial discharge tests would indicate that the shape of the storage tank should not vary widely from that tested here; that is, if ice is stored over a larger area than that directly under the water distribution header, there may be some difficulty in fully melting the tank.

The power consumption of the unit proved to be much greater than that related in the Turbo literature. The main contributors to this difference were determined to be the motor efficiency, allowable margins in compressor rating data, and the nonsteady nature of the compressor operations.

REFERENCES

1. T. K. Stovall and J. J. Tomlinson, *Commercial Cool Storage Laboratory Test Procedure*, ORNL/TM-11511, Martin Marietta Energy Systems, Inc., Oak Ridge Natl. Lab., May 1990.

2. T. K. Stovall, *Ice-Storage Efficiency Considerations*, ORNL/TM-11678, Martin Marietta Energy Systems, Inc., Oak Ridge Natl. Lab., to be published.

3. Turbo Refrigerating Company, *Thermal Storage Ice Harvesting for Air Conditioning and Process Cooling*, Bulletin TE-20, Turbo Refrigerating Company, Denton, TX 76201, 1986.

4. 1986 ASHRAE Handbook, *Refrigeration Systems and Applications*, American Society of Heating, Refrigerating and Air Conditioning Engineers, Inc., Atlanta, Ga., 1986.

5. *Micro Motion Model D Mass Flow Meters Instruction Manual*, 1000572-2-87, Micro Motion, Inc., Boulder, Colo., February 1987.

6. Engineering Application Data, Model CG, Royce Industrial Compressor Division, EADCG-1A, ECC Corporation, Hauppauge, N.Y.

7. Snomax™ (snow inducer), Advanced Genetic Sciences, Oakland, Calif.

8. G. T. Kartsounes and R. A. Erth, "Computer Calculation of the Thermodynamic Properties of Refrigerants 12, 22 and 502," *ASHRAE paper No. 2200*, presented at ASHRAE Annual Meeting, Washington D.C., August 22—25, 1971.

9. *SAS User's Guide: Statistics*, Version 5 Edition, SAS Institute Inc., Cary, N.C., 1985.

10. Turbo drawing 8615706 (Sht 2 of 2), Turbo Refrigerating Company, Denton, Tex.

Appendix

ISTF INSTRUMENTATION

Data Acquisition and Control

A data acquisition system and computer are used to control the thermal loading rate, the water pump speed, recirculation valve positions, and the condensation temperature, and to collect the data from system instrumentation. The computer allows short sampling times of the instrumentation to provide data for detailed analysis and feedback during transient system operation. Direct controls, outside of the data acquisition/computer system, are available for booster pump operation and auxiliary portions of the test facility.

Temperature Measurements

Refrigerant temperature measurements are made by RTDs bonded to the outside of the copper pipes. These RTDs were calibrated by the manufacturer to 0.3°F. After installation, the recorded refrigerant temperatures were compared to the expected thermodynamic states for the corresponding pressure measurements. Water temperature measurements are made by RTDs inserted into the PVC pipes. These RTDs are calibrated by the manufacturer to ± 0.5°F and checked against an ice bath after installation. The RTDs were also checked against each other under conditions where an unloaded heat exchanger, for example, would be expected to show the same inlet and outlet temperature. The RTD calibrations are periodically rechecked, and instruments that have drifted beyond 0.5°F are replaced.

Flow Measurements

Vortex-shedding flowmeters are used to measure the condenser cooling water flow, the water flow to the heater, and the water flow to the ice tank. The vortex-shedding refrigerant flowmeter imposes a pressure drop of ~ 0.5 psia. These flowmeters are accurate to $\pm 0.8\%$ of the reading for liquid flows. The flowmeters used to measure water volumetric flow were checked after installation by running water through the lines into a 55-gal drum placed on a scale.

The Coriolis mass flowmeters used to measure liquid and gaseous refrigerant mass flows were calibrated by the manufacturer to $\pm 0.4\%$ of full scale, which is 1000 lb/min. Also,

energy balances on the condenser and evaporator can be used to assess the continued accuracy of these devices.

Pressure Measurements

Refrigerant pressure measurements are made with pressure transducers to allow the electronic recording of the values. The accuracy of these absolute pressure readings is rated at $\pm 0.11\%$ of full scale. However, the calibration certificates supplied with each transducer show accuracies of $\pm 0.004\%$ or better. Also, the transducer calibration was rechecked after installation and periodically thereafter using laboratory calibration equipment. The pressure transducers located in the high-pressure portion of the loop, that is, between the compressor discharge and the expansion valve, are rated for 0 to 500 psia. All others are rated for 0 to 250 psia. During testing, the pressure measurements are periodically compared to other measurements within the loop and to the expected refrigerant properties.

Electrical Measurements

Electrical measurements for the compressor motor power (rated at 40 hp), circulating pump(s) power (from 2 to 5 hp), and heater power (0 to 135 kW) are measured by watt/watt-hour transducers. The watt-hour measurements are accurate to $\pm$[0.2% of the reading + 0.01% of the rated output)/(power factor)]. The watt-hour meters for the compressor motor was checked by measuring the voltage and current on each of three phases of the nominal 440-V delta connection. The watt-hour meter for the heater was checked by comparison to the heat absorbed by the water as measured by the flow and temperature change. The accuracy of this heater's watt-hour meter is poor because of the semiconductor controlled rectifier (SCR), or phase angle power controller, used to vary the heater power. Heater energy use measurements are therefore based on the fluid flow rate and temperature change, although the power consumption is recorded as an additional check.

ORNL/TM-11657
Dist. Category UC-202

Internal Distribution

1. T. D. Anderson
2. V. D. Baxter
3. S. H. Buechler
4. R. S. Carlsmith
5. W. G. Craddick
6. P. D. Fairchild
7. D. J. Fraysier
8. W. Fulkerson
9. R. B. Honea
10. J. E. Jones Jr.
11. L. Jung
12. R. J. Kedl
13. M. A. Kuliasha
14. W. A. Miller
15. W. R. Mixon
16. M. Olszewski
17. A. E. Ruggles
18. A. C. Schaffhauser
19. M. Siman-Tov

20-29. T. K. Stovall

30. J. J. Tomlinson
31. C. D. West
32. G. L. Yoder
33. ORNL Patent Section
34. Central Research Library
35. Document Reference Section

36-37. Laboratory Records Department

38. Laboratory Records (RC)

External Distribution

39. John Stephen Anderpont, Chicago Bridge & Iron Company, 800 Jorie Boulevard, Oak Brook, IL 60522-7001
40. Debra L. Catanese, P.E., Pennsylvania Electric Company, 311 Industrial Park Rd., Johnstown, PA 15904
41. Tom Carter, Baltimore Aircoil Company, P.O. Box 7322, Baltimore, MD 21227
42. Russ Eaton, Director, Advanced Utility Concepts Division, U.S. Department of Energy, Forrestal Building, CE-142, 1000 Independence Avenue, Washington, DC 20585
43. Imre Gyuk, Office of Energy Storage and Distribution, U.S. Department of Energy, Forrestal Building, CE-32, 1000 Independence Avenue, Washington, DC 20585
44. Landis Kannberg, Battelle Pacific Northwest Laboratories, P.O. Box 999, Battelle Boulevard, Richland, WA 99352
45. Don Kemp, Turbo Refrigerating Company, 1815 Shady Oaks Drive, P.O. Box 396, Denton, TX 76202
46. K. W. Klunder, Director, Office of Energy Management, Department of Energy, CE-14, Forrestal Building, 1000 Independence Avenue, Washington, DC 20585
47. Dave Knebel, Paul Mueller Company, P.O. Box 828, Springfield, MO 65801-0828
48. David Laybourn, P.E., Director of Marketing, Reaction Thermal Systems, Inc., 840 Latour Court, Suite A, Napa, CA 94558
49. George Manthey, DOE, Oak Ridge Operations, Oak Ridge, TN 37831
50. Robert P. Miller, Baltimore Aircoil Company, P.O. Box 7322, Baltimore, MD 21227
51. Tony Min, Mechanical Engineering Department, North Carolina Agricultural and Technical State University, Greensboro, N.C. 27411

52. Victor A. Needham III, Marketing Programs Director, Cincinnati Gas & Electric Company, P.O. Box 960, Cincinnati, OH 45201
53. Dave Pellish, U.S. Department of Energy, Forrestal Building, MS CE-332, Room 5H-79, 100 Independence Avenue, Washington, DC 20585
54. Veronika A. Rabl, Electric Power Research Institute, 3412 Hillview Avenue, P.O. Box 10412, Palo Alto, CA 94303
55. Eberhart Reimers, Advanced Utility Concepts Division, U.S. Department of Energy, Forrestal Building, CE-142, 1000 Independence Avenue, Washington, DC 20585
56. Richard Rhodes, FAFCO, Inc., 235 Constitution Drive, Menlo Park, CA 94025
57. Marwan Saliba, Energy Engineering Institute, Dept. of Mechanical Engineering, San Diego State University, San Diego, CA 92182-0191
58. Brian Silvetti, Calamac Manufacturing Corporation, Box 710, 150 South Van Brunt Street, Englewood, NJ 07631
59. Robert L. San Martin, Deputy Assistant Secretary, Office of Utility Technology, Department of Energy, CE-10, 6C-026/Forrestal Bldg., 1000 Independence Avenue, Washington, DC 20585
60. Chang W. Sohn, U.S. Army Corps of Engineers, P.O. Box 4005, Champaign, IL 61824-4005
61. Laura Thomas, Marketing Manager, York International Corporation, P.O. Box 1592, York, PA 17405-1592
62. Samuel G. Tornabene, Edison Electric Institute, 1111 19th Street, N.W., Washington, DC 20036-3691

63-72. R. D. Wendland, Electric Power Research Institute, 3412 Hillview Avenue, Box 10412, Palo Alto, CA 94303

73. Maurice W. Wildin, Professor, The University of New Mexico, Department of Mechanical Engineering, Albuquerque, NM 87131
74. Office of Assistant Manager for Energy Research and Development, Department of Energy, ORO, Oak Ridge, TN 37831

75-86. Given distribution as shown in DOE/OSTI-4500-R75 under Category UC-202 (Thermal Energy Storage)